

Making the Grid Truly Smart: Autonomous System Identification in “Modemless” DC MicroGrids

Marko Angjelichinoski, *Student Member, IEEE*, Anna Scaglione, *Fellow, IEEE*, Petar Popovski, *Fellow, IEEE*, Čedomir Stefanović, *Member, IEEE*

Abstract—We introduce novel framework for autonomous learning of the own configuration in direct current (DC) MicroGrids (MG) with high penetration of power electronic converters and without access to an external communication system. The framework is implemented within the decentralized primary droop control loop, enabling the controllers to learn (i) the generation capacities of dispatchable power sources, (ii) the load demands, and (iii) the admittances of the distribution system lines. Its development is founded on the fact that the steady state bus voltages in droop-controlled MG depend on the generation capacities, the load and the admittance matrix of the distribution system, through a non-linear, implicit model that can be estimated via asymptotically efficient Maximum Likelihood Estimation procedure. To define a well-conditioned estimation problem, we employ solution based on the concept of decentralized, coordinated training where the primary droop controllers temporarily switch between operating points, following a protocol that relies on predefined, amplitude-modulated training sequences. The numerical evaluations verify the analysis and confirm the practical potential of the framework.

Index Terms—MicroGrids, droop control, training sequences, bus signaling, Maximum Likelihood Estimation

I. INTRODUCTION

MICROGRIDS (MGs) are localized clusters of loads and small-scale distributed energy resources (DERs) [1]. Lately, MG research and development are experiencing a significant momentum, as the future smart grid is envisioned as a mesh of interconnected autonomous MG systems. In this respect, low voltage direct current (LVDC) MGs are considered as a solution for residential areas due to the flexibility of the control, the absence of reactive power component and the seamless integration with DC renewable generation, DC energy storage systems and DC smart loads [2], [3].

A distinguishing characteristic of MGs is the use of programmable *power electronic converters* (PECs) to connect the DERs to the MG distribution system. PECs allow for software implementation of advanced control mechanisms, thereby significantly increasing the flexibility and modularity of the MG control [2], [3]. The MG control plane is divided into (fast) primary and (slower) upper control layer [3], [4]. The primary control deals with high frequency dynamic compensation and state regulation; it is decentralized and standardly implemented

in the form of *droop control*, where each controller relies only on its local voltage/current measurements [3], [4]. The upper control layers provide optimized control references for the primary control layer and can be implemented in centralized or distributed fashion, operating with significantly lower frequency than the primary control layer [5]–[10]. A ubiquitous upper-layer control application is the *optimal power flow (OPF)*: its goal is to compute the optimal droop control references that minimize the total generation cost while keeping the load balanced [6]–[8].

The standard assumption is that the feedback of the upper control layer is closed via an external communication system [3], [6], [8]. However, this approach was challenged recently due to several issues [2], [3]. First, the distributed power systems, particularly MGs, are dynamic, sporadic and ad-hoc in nature, thus the installation of external communication system may prove impractical and cost inefficient. Second, the very principle of MG self-sustainability disapproves of using external systems to drive MG operation. In particular, an external communication system may reduce the efficiency of the MG due to its limited reliability and availability. Last but not least, there is a growing concern about the cyber-security of power systems that exploit external communications, as the related security threats and attacks might severely compromise the stability and operation of the power system even if firewalls are erected for its protection, leading to blackouts, equipment damage and investment losses [11], [12].

In this paper, we propose a “modemless” framework for the acquisition of the information required for the operation of the DC MG upper control layer, i.e., a framework that does not depend on an external communication system. The mandatory upper control layer information comprises i) the generation capacities of the dispatchable DERs, ii) the demands of the loads, and iii) the admittance matrix of the distribution network [7]. Our motivation is driven by the fact that the state of the MG, represented by the bus voltages, is inherently parametrized by the generation capacities, load demands, and line admittances through a non-linear, implicit model. Hence, the information required by the upper control layer can be estimated from local voltage observations. To do so, the PECs deliberately move the MG through a sequence of sub-optimal operating states via coordinated and amplitude-modulated perturbations of the droop control parameters, referred to as training sequences. This way, PECs create sequence of local bus voltage measurements from which the required information can be uniquely estimated via Maximum Likelihood Estimation (MLE) procedure, provided that the training sequences satisfy sufficiency criteria. The

M. Angjelichinoski, P. Popovski and Č. Stefanović are with the Department of Electronic Systems, Aalborg University, Denmark (e-mail: {maa.petarp,cs}@es.aau.dk). A. Scaglione is with the School of Electrical, Computer and Energy Engineering, Arizona State University, AZ, USA (e-mail: Anna.Scaglione@asu.edu).

The work presented in this paper was supported in part by EU, under grant agreement no. 607774 “ADVANTAGE”.

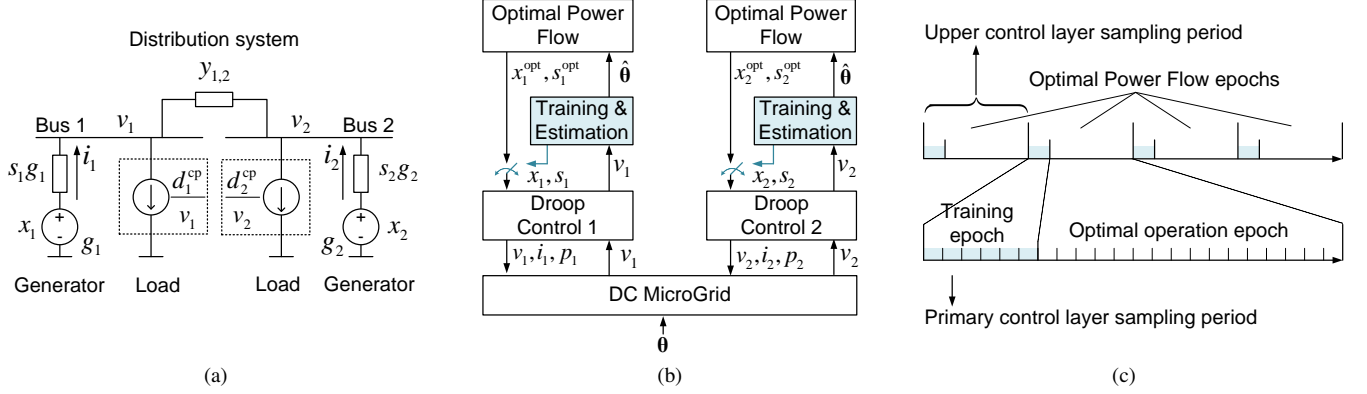


Fig. 1. Motivating example and overview of the proposed framework: (a) steady state diagram of an example DC MG with two buses, two droop-controlled generators and two non-linear loads, (b) identification via primary control for performance optimization of the example DC MG, (c) temporal organization of the proposed operational protocol.

proposed framework exploits the signal processing capabilities of the PECs, drawing from the reliability/availability/security of the MG itself and requires only software modifications in order to be implemented. The evaluations show that in LVDC MG configurations with less than 10 buses, the relative estimation error can be kept within 1% margin using tolerably small voltage deviations.

The rest of the paper is organized as follows. This section concludes with an overview of the notation used in the manuscript. Section II presents the motivation and the contributions of the paper, also briefly reviewing the related literature. Section III introduces the general model of DC MG systems. Section IV introduces the decentralized training architecture. Section V is the pivotal section of the paper, presenting our solution to the estimation problem. Section VI assesses the performance of the proposed solution, verifying its potential. Section VII concludes the paper.

Notation: An ordered set of non-negative integers is denoted by a calligraphic letter, and the corresponding uppercase italic letter denotes its cardinality, e.g. \mathcal{N} and $|\mathcal{N}| = N$. Column vectors and matrices are denoted by lowercase and uppercase bold letters, e.g., $\mathbf{a} \in \mathbb{R}^{N \times 1}$ and $\mathbf{A} \in \mathbb{R}^{N \times M}$. $\mathbf{a}_{-n} \in \mathbb{R}^{(N-1) \times 1}$ is obtained from \mathbf{a} by removing the element at position n . Similarly, $\mathbf{A}_{-m} \in \mathbb{R}^{N \times (M-1)}$ is obtained from \mathbf{A} by removing the m -th column \mathbf{a}_m . $(\cdot)^T$, $(\cdot)^\dagger$, $\text{vec}(\cdot)$, $\text{dim}(\cdot)$ and $\text{rank}(\cdot)$ denote the transpose, the pseudo-inverse, the vectorization, the dimension and the rank of the argument. \otimes denotes the Kronecker product while \odot and \oslash denote the Hadamard (element-wise) product and division of vectors/matrices of adequate dimensions. The vectors $\mathbf{1}_N$, $\mathbf{0}_N$ and \mathbf{e}_n , $n \in \mathcal{N}$, denote the all-ones, all-zeros and the principal coordinate vector, whilst, \mathbf{I}_N and $\mathbf{0}_{N \times N}$ denote the $N \times N$ identity and all-zero matrices. $\text{D}(\mathbf{a})$ denotes diagonal matrix with the entries of \mathbf{a} on the main diagonal. We frequently use the identity $\text{vec}(\text{D}(\mathbf{a})) = \mathbf{O}_N \mathbf{a}$ where the $N^2 \times N$ matrix $\mathbf{O}_N = \sum_{n \in \mathcal{N}, |\mathcal{N}|=N} \mathbf{e}_n \otimes (\mathbf{e}_n \mathbf{e}_n^T)$. $\nabla_{\text{var}}(\cdot)$ denotes the derivative of the argument (scalar/vector) w.r.t. “var” (scalar/vector); we employ numerator layout for multivariable calculus. The pdf of Gaussian random variable/vector is denoted with $\mathcal{N}(\text{“mean”}, \text{“(co)variance”})$.

II. MOTIVATION, CONTRIBUTIONS AND RELATED WORK

Motivating Example: Consider the DC MG system depicted in Fig. 1(a). There are two buses connected via distribution line with admittance $y_{1,2}$. Bus n , $n \in \{1, 2\}$, interfaces a DER with generation capacity g_n and non-linear constant power load with demand d_n^{cp} . The bus voltage v_n is controlled by the DER n via decentralized droop control law $v_n = x_n - (s_n g_n)^{-1} i_n$ driven by the output current i_n . The controllable parameters x_n and s_n are the *reference voltage* and the *droop slope*, respectively [3]. For a given configuration of droop controllers, generation capacities, load demands and topology (referred to as operating point), the MG steady state is uniquely characterized by v_1 and v_2 . Applying the Kirchhoff’s laws in steady state, we obtain the system of power flow equations:

$$s_n g_n v_n (x_n - v_n) = d_n^{cp} + y_{n,m} v_n (v_n - v_m), \quad (1)$$

where $s_n g_n v_n (x_n - v_n) = v_n i_n = p_n$ is the power injected by the DER n and $y_{n,m} v_n (v_n - v_m)$ is the power that flows between buses $n, m \in \{1, 2\}$. The system (1) can be written compactly via the following non-linear vector equation:

$$\omega(\mathbf{v}, \mathbf{x}, \mathbf{s}, \boldsymbol{\theta}) = \mathbf{0}, \quad (2)$$

where $\mathbf{v} = [v_1, v_2]^T$ is the vector of the steady state bus voltages, $\mathbf{x} = [x_1, x_2]^T$ and $\mathbf{s} = [s_1, s_2]^T$ are the droop control vectors, and $\boldsymbol{\theta} = [g_1, g_2, d_1^{cp}, d_2^{cp}, y_{1,2}]^T$ the *parameter vector*.

The optimized values of the primary control parameters \mathbf{x} and \mathbf{s} are provided by an upper control layer optimization, e.g., by OPF. Let $\mathbf{p} = [p_1, p_2]^T$ denote the dispatch policy vector. Then, the basic variant of the OPF for the droop-controlled MG can be formulated as the following minimization problem:

$$\begin{aligned} \min_{\mathbf{x}, \mathbf{s}, \mathbf{v}} \{c(\mathbf{p})\} \\ \text{s.t. } \omega(\mathbf{v}, \mathbf{x}, \mathbf{s}, \boldsymbol{\theta}) = \mathbf{0}, \end{aligned} \quad (3)$$

where the power generation cost function $c(\mathbf{p})$ is assumed to be a priori know.¹ The focus of the paper is not on

¹In MGs, the cost function is assumed to be separable and linear [6], i.e., $c(\mathbf{p}) = a_1 p_1 + a_2 p_2$; in such case, the positive costs per unit generated power a_1 and a_2 are known to each DER.

solving (3), rather, we are interested in designing an approach where each controller locally obtains the information that is necessary to solve such a problem *without* using an external communication system. To this end, we observe that (3) can be readily solved when the generation capacities g_1, g_2 , the load demands $d_1^{\text{cp}}, d_2^{\text{cp}}$ and the distribution system topology $y_{1,2}$ (i.e., θ) are known. This is evident from (3), as θ parametrizes the objective and the constraint. On the other hand, note that from (1) and (2), the bus voltages v_1 and v_2 , depend on θ as well. Therefore, θ can be *estimated* from local observations of v_1 and v_2 and used to solve (3).

Contributions: The proposed estimation framework in the context of the motivating example is illustrated in Fig. 1(b), and its temporal organization in Fig. 1(c). The controllers are assumed to be synchronized, periodically sampling the system state.² The framework features periodically recurring training epochs; we assume that θ changes at the beginning of each OPF epoch and remains fixed until the next epoch [6]–[8].³ At the start of each epoch, θ changes randomly and independently from the previous epochs, such that we assume that there is no prior knowledge of the process governing its dynamics and use classical, non-Bayesian estimation framework.⁴ The analysis is performed for a single OPF epoch for which θ is modeled as deterministic unknown parameter vector. We adopt decentralized identification architecture, where each DER estimates θ by processing only local bus voltage measurements, see Fig. 1(c). The main contributions of the paper can be summarized as follows:

- We develop a detailed model of droop-controlled DC MG with multiple buses and characterize the dependence of the steady state bus voltages on the droop control parameters, the generation capacities, the load demands and the admittance matrix of the distribution system.
- We design a decentralized training protocol for the training epochs during which the droop controllers synchronously “inject” small and predefined droop parameter perturbations i.e., training sequences.
- As a benchmark, we first analyze the ideal case when each controller acquired the bus voltage measurement sequences of all other controllers (e.g., through some ideally-performing external network) and derive MLE algorithm with the corresponding Cramer-Rao lower bound (CRLB).
- We consider the case when the controllers observe their local measurement sequence and exchange the observed information among themselves *also* via dedicated sequences of droop control perturbations. In other words,

²If the PECs are equipped with an external synchronization interface, like GPS, the synchronization is easily achieved. Otherwise, PECs can rely on their internal clocks for coarse synchronization, and then apply standard techniques to achieve and maintain precise synchronization, e.g., use of synchronization preambles, adequate signaling formats, etc.

³In practice θ changes infrequently, implying that the required frequency of the OPF epochs is significantly smaller than the sampling frequency of the primary control [3], see Fig. 1(c).

⁴This assumption, besides allowing to model wide range of generation/demand conditions in a unified manner (without relaying on elaborate prior models), forms the basis for the development of sophisticated Bayesian-based identification and tracking procedures. Such extensions are outside the scope of the paper and part of our on going investigations.

the droop control perturbations are used *both* for the generation of the local observations and their exchange among PECs. In the latter case, the relation between the droop control perturbations and the incurred bus voltage deviations is interpreted as the input-output relation of an implicit communication channel. The controllers then *modulate* the local bus voltage measurements into the amplitude of the droop control perturbations, enabling each controller to estimate θ like in the benchmark case.

Literature Review: Recent works in MG control suggest using the existing power electronic equipment and powerlines as means for communication.⁵ Such solution for DC MGs, termed *bus signaling* has been proposed in [14], in which each PEC unit measures the output voltage and if the voltage crosses predefined threshold, the units take predefined actions. Subsequently, bus signaling was applied in a variety of MG settings [15], [16]. However, this approach is MG configuration-dependent and performs well in small, controlled environments with only few DERs, serving dedicated load which can be easily predicted, but is not suitable for dynamic and modular MGs.

The idea of using droop control perturbations to disseminate information among MG units via bus voltage deviations was introduced in [17], under the name of power talk. The works that followed focused on designing power-talk strategies for reliable communication, investigation of its fundamental properties and its applications [18]–[21]. The proposed information embedding and dissemination technique in this paper can be viewed as a variant of power talk communication.

Decentralized training is widely used in communication systems for channel estimation [22]. Recently, it was also applied in MGs for estimation of the parameters of the Thevenin/Norton equivalent circuit, under the name of *active impedance estimation* [23], [24]. However, this approach is of a limited application scope; namely, only one controller disturbs the system as a time to estimate few parameters of interest, such as the grid impedance [23], [24]. In contrast, in our work, multiple units simultaneously train the system with an aim to extract all information that is necessary to support the autonomous operation of the upper control layer.

III. SYSTEM MODEL

In this section, we introduce a general model (Section III-A) and characterize the steady-state operation of a droop controlled DC MG (Section III-B).⁶

A. General Multiple-Bus DC MicroGrid

1) *Buses, Distributed Energy Resources and Loads:* A DC MG is a collection of DERs and loads, connected to low voltage LVDC distribution system, see Fig. 2. The distribution system consist of $N \geq 1$ buses, indexed in the set $\mathcal{N} = \{1, \dots, N\}$, and interconnected via distribution lines. Each bus n is modeled as a node in the MG characterized

⁵Standard powerline communication systems (PLC) are regarded as external to MG, as they require installation of dedicated PLC modems [13].

⁶All voltages, currents, powers and admittances in DC MGs are reals.

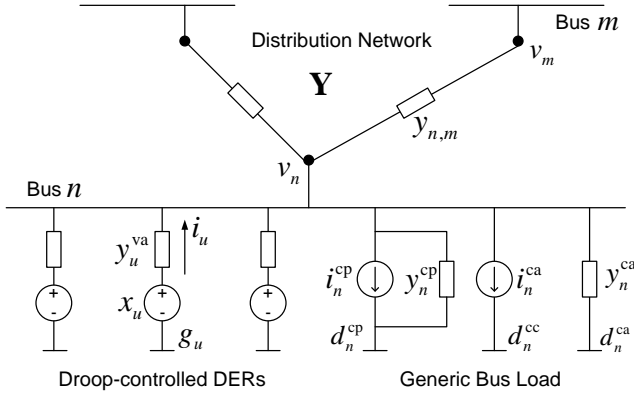


Fig. 2. System model: general multiple-bus DC MG in steady state.

by a steady state voltage v_n , $n \in \mathcal{N}$, and all DERs and loads connected to bus n measure the same voltage v_n . The bus voltages are collected in the vector $\mathbf{v} = [v_1, \dots, v_N]^T$. The distribution line connecting buses n and m is characterized by an admittance $y_{n,m}$, where $y_{n,m} \equiv y_{m,n} \geq 0$, and where equality holds if buses n and m are not directly connected, or if $n = m$. We define the $N \times N$ admittance matrix \mathbf{Y} as:

$$[\mathbf{Y}]_{n,m} = \begin{cases} \sum_{j \in \mathcal{N}} y_{n,j}, & n = m, \\ -y_{n,m}, & n \neq m, \end{cases} \quad (4)$$

for $n, m \in \mathcal{N}$. Observe that \mathbf{Y} is fully specified by the supra-diagonal elements. We organize these elements in a vector $\psi = [\dots, y_{n,m}, \dots]^T$, $n, m \in \mathcal{N}$, $m > n$, with dimension $\dim(\psi) = \frac{1}{2}N(N-1) \times 1$. Using ψ , the admittance matrix can be written as the weighted Laplacian $\mathbf{Y} = \mathbf{A}\mathbf{D}(\psi)\mathbf{A}^T$, where \mathbf{A} is the $N \times \dim(\psi)$ oriented incidence matrix, defined as $\mathbf{A} = [\dots, \mathbf{a}_{n,m}, \dots]^T$, $n, m \in \mathcal{N}$, $m > n$; the elements of the columns $\mathbf{a}_{n,m}$ are given by:

$$[\mathbf{a}_{n,m}]_j = \begin{cases} 1, & j = n, \\ -1, & j = m, \\ 0, & \text{otherwise,} \end{cases} \quad (5)$$

for $j \in \mathcal{N}$.

The total number of DERs connected to the MG is U and they are indexed in the ordered set $\mathcal{U} = \{1, \dots, U\}$. The DERs use PECs to interface the distribution system and their outputs (voltage and current) are locally controlled through decentralized primary controllers. The output current and the power generation capacity of DER $u \in \mathcal{U}$ are denoted by i_u and g_u , respectively. Bus n hosts U_n DERs, $0 < U_n < U$, i.e., the set \mathcal{U} is split into N disjoint subsets, denoted by \mathcal{U}_n , $|\mathcal{U}_n| = U_n$. We introduce the related bus-DER correspondence matrix $\mathbf{Q} \in \{0, 1\}^{U \times N}$ with elements:

$$[\mathbf{Q}]_{u,n} = \begin{cases} 1, & u \in \mathcal{U}_n, \\ 0, & \text{otherwise,} \end{cases} \quad (6)$$

for $n \in \mathcal{N}$, $u \in \mathcal{U}$. Note that $\text{rank}(\mathbf{Q}) = N$. In the rest of the paper, we assume that \mathbf{Q} is known a priori.

Bus $n \in \mathcal{N}$ also hosts a collection of loads, represented through an aggregate model as a mixture of three components [25]: 1) *constant admittance* $y_n^{\text{ca}} = x^{-2}d_n^{\text{ca}}$, 2) *constant current* $i_n^{\text{cc}} = x^{-1}d_n^{\text{cc}}$, and 3) *constant power* component d_n^{cp} . The

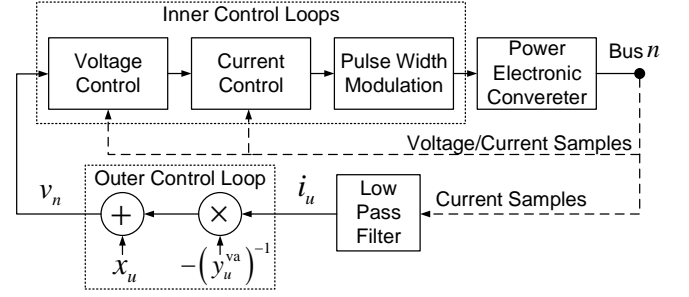


Fig. 3. Block diagram of a droop-controlled VSC unit $u \in \mathcal{U}_n$.

quantities d_n^{ca} , d_n^{cc} and d_n^{cp} are the rated power demands of the components at the rated voltage x of the MG. For a given d_n^{cp} , the constant power component is approximated with an equivalent positive current source in parallel with negative admittance, with the electrical parameters [3]:

$$i_n^{\text{cp}} \approx \frac{2d_n^{\text{cp}}}{v_n}, \quad y_n^{\text{cp}} \approx -\frac{v_n^2}{d_n^{\text{cp}}}. \quad (7)$$

The load components are collected in separate $N \times 1$ vectors: $\mathbf{d}^{\text{ca}} = [d_1^{\text{ca}}, \dots, d_N^{\text{ca}}]^T$, $\mathbf{d}^{\text{cc}} = [d_1^{\text{cc}}, \dots, d_N^{\text{cc}}]^T$ and $\mathbf{d}^{\text{cp}} = [d_1^{\text{cp}}, \dots, d_N^{\text{cp}}]^T$. The $3N \times 1$ load demand vector is defined as $\mathbf{d} = [(\mathbf{d}^{\text{ca}})^T, (\mathbf{d}^{\text{cc}})^T, (\mathbf{d}^{\text{cp}})^T]^T$.

2) *Primary Control*: A common primary control configuration for electronically controlled DER units is the *Voltage Source Converter (VSC)*, see Fig. 3. The objective of a VSC unit is to regulate the output voltage and current (i.e., output power) of the DER as the loads in the system change, and to maintain fair power sharing among the DERs. A *decentralized* control architecture of a VSC comprises fast inner and slower outer control loops. The inner control loop consists of current and voltage control channels with bandwidth of the order of several tens of kHz, equal to the sampling frequency of the converter ϕ_S . Their role is to maintain the output bus voltage v_n and the output current i_u of unit $u \in \mathcal{U}_n$ to specific reference values. The outer control loop is closed via filtered current feedback, and is slower than the inner control loops by an order of magnitude. The current feedback generates the reference value for the inner voltage control channel, via the following steady state control law, see Fig. 3:

$$v_n = x_u - \frac{1}{y_u^{\text{va}}} i_u, \quad u \in \mathcal{U}_n, \quad n \in \mathcal{N}. \quad (8)$$

This implementation is known as the decentralized droop control [3], [4]. The droop controller has two controllable parameters: the reference voltage x_u that determines the voltage rating of the system and the virtual admittance y_u^{va} that determines the power sharing among units. In practice, the value of the virtual admittance is set to enable fair proportional power sharing, based on the power capacities of the units [3]:

$$y_u^{\text{va}} = s_u g_u. \quad (9)$$

s_u is the droop slope of unit u that is standardly set as [3]:

$$s_u = (v_{\min}(x_u - v_{\min}))^{-1}, \quad (10)$$

satisfying $v_n \geq v_{\min}$, $\forall n \in \mathcal{N}$ where v_{\min} is the minimal allowable voltage that the system is designed to tolerate. In

$$\omega = D(\mathbf{v})D\left(\mathbf{Q}^T D(\mathbf{g})\mathbf{s} + \frac{1}{x^2}\mathbf{d}^{\text{ca}}\right)\mathbf{v} + D(\mathbf{v})\mathbf{Y}\mathbf{v} - D(\mathbf{v})\left(\mathbf{Q}^T D(\mathbf{g})(\mathbf{x} \odot \mathbf{s}) - \frac{1}{x}\mathbf{d}^{\text{cc}}\right) + \mathbf{d}^{\text{cp}}. \quad (14)$$

steady state, the droop-controlled VSC units are modeled as voltage sources in series with the virtual admittance, see Fig. 2.⁷ The generation capacities and the droop controllers' configuration parameters are collected in $U \times 1$ vectors $\mathbf{g} = [g_1, \dots, g_U]^T$, $\mathbf{x} = [x_1, \dots, x_U]^T$ and $\mathbf{s} = [s_1, \dots, s_U]^T$.

3) *Parameter Vector*: We organize \mathbf{g} , \mathbf{d} and ψ into a *deterministic parameter vector*, denoted with θ , as follows:

$$\theta = [\mathbf{g}^T, \mathbf{d}^T, \psi^T]^T, \quad (11)$$

with dimension $\dim(\theta) = (U + \frac{1}{2}N(N+5)) \times 1$.

B. Steady State Equations

Let $\mathbb{X} \subset \mathbb{R}^U$, $\mathbb{S} \subset \mathbb{R}^U$ denote the sets of primary controllers that maintain the steady state bus voltages within the bounded set $\mathbb{V} \subset \mathbb{R}^N$ for any value of θ .⁸ Furthermore, as no prior knowledge on θ is assumed, we let $\theta \in \mathbb{R}^{\dim(\theta)}$. We refer to a point in $\mathbb{X} \times \mathbb{S} \times \mathbb{R}^{\dim(\theta)}$ as *operating point*; the steady state bus voltages for any operating point are obtained via:

$$\mathbf{v} = \mathbf{f}(\mathbf{x}, \mathbf{s}, \theta), \quad (12)$$

where $\mathbf{f} : \mathbb{X} \times \mathbb{S} \times \mathbb{R}^{\dim(\theta)} \mapsto \mathbb{V}$, $\mathbf{f} = [f_1, \dots, f_N]^T$ is a non-linear mapping in general, characterized with the following proposition:

Proposition 1. *The DC MG system in steady state is characterized by the implicit power balance equation:*

$$\omega(\mathbf{v}, \mathbf{x}, \mathbf{s}, \theta) = \mathbf{0}_N, \quad (13)$$

where $\omega : \mathbb{V} \times \mathbb{X} \times \mathbb{S} \times \mathbb{R}^{\dim(\theta)} \mapsto \mathbb{R}^N$, and $\omega = [\omega_1, \dots, \omega_N]^T$ is given in (14).⁹

The power balance equation (13) is quadratic in \mathbf{v} . For any operating point for which the Jacobian $\nabla_{\mathbf{v}}\omega$ is full rank, the implicit function theorem guarantees the existence of \mathbf{f} as the unique solution of (13); however, obtaining this solution in closed form is out of reach [26]. The non-linear nature of (13) stems from the presence of constant power loads \mathbf{d}^{cp} [26]. When $\mathbf{d}^{\text{cp}} = \mathbf{0}_N$, the DC MG, (14) obtains the form:

$$\left(D\left(\mathbf{Q}^T D(\mathbf{g})\mathbf{s} + \frac{1}{x^2}\mathbf{d}^{\text{ca}}\right) + \mathbf{Y}\right)\mathbf{v} = \mathbf{Q}^T D(\mathbf{g})(\mathbf{x} \odot \mathbf{s}) - \frac{1}{x}\mathbf{d}^{\text{cc}}, \quad (15)$$

⁷Another common primary control architecture is in the form of *Current Source Converter (CSC)*, where the voltage control loop is absent and the outer control loop generates the current reference value via the Maximum Power Point Tracking algorithm, injecting the maximum available power [3]. In steady state, CSC is modeled as a constant power source via a negative current source and parallel admittance, as in (7) but with opposite signs. Assuming that bus n , also hosts CSC units with total power injection g_n^{CSC} , it can be easily shown that the presence of the CSC simply reduces the constant power component of the bus load, i.e., $d_n^{\text{cp}} - g_n^{\text{CSC}}$. Thus, from architectural perspective, CSC units are equivalent to constant power load with negative consumption, confirming the generality of our system model.

⁸Typical constraints that determine the sets \mathbb{X} , \mathbb{S} and \mathbb{V} are the converters' dynamic ranges on the output voltage ripple $v_{\min} \leq v_n \leq v_{\max}$ and output current rating $0 \leq i_u \leq \frac{g_u}{v_{\min}}$ for $u \in \mathcal{U}$, $n \in \mathcal{N}$ [3], [17]–[20].

⁹In the rest of the paper, we omit denoting explicitly the dependence of ω on \mathbf{v} , \mathbf{x} , \mathbf{s} , θ .

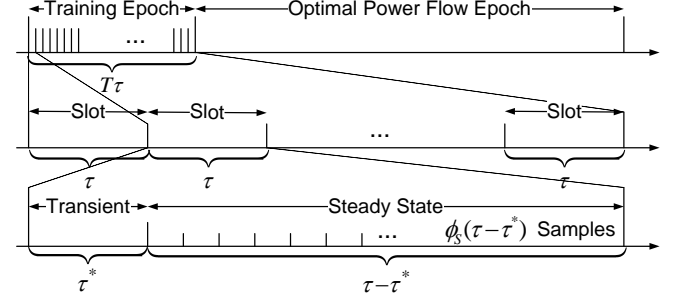


Fig. 4. Training epoch organization.

and \mathbf{v} is the unique solution to a linear equation.

IV. TRAINING EPOCH

The pivotal problem is one of decentralized system identification where an arbitrary controller k , connected to arbitrary bus m , identifies an unknown parameter vector θ_{-k} representing the exogenous MG input that parametrizes its state, i.e., the bus voltages (the formal definition is presented in Section V). To make θ_{-k} uniquely identifiable, the controllers utilize a decentralized training protocol, synchronously perturbing the droop parameters according to predefined training sequences, as described next.

A. Training Protocol and Training Sequences

As outlined in Section III-B, the time axis is divided into periods, each of them consisting of a training epoch and an OPF epoch, see Fig. 1(c) and Fig. 4. The training epoch is further divided into slots of duration τ . We index each slot with $t \in \mathcal{T} = \{0, \dots, T-1\}$. The slot duration complies with the control bandwidth of the droop control loop, allowing the bus to reach a steady state after transient time τ^* , $\tau^* \ll \tau$, yielding $\phi_s(\tau - \tau^*)$ voltage samples per slot for each controller.

In slot t , all units simultaneously perturb their local droop control parameters, according to perturbation signals $x_u(t)$, $s_u(t)$, $u \in \mathcal{U}$. The perturbation signals are organized in $T \times U$ training matrices \mathbf{X} , \mathbf{S} , defined as $[\mathbf{X}]_{t,u} = x_u(t)$ and $[\mathbf{S}]_{t,u} = s_u(t)$, $u \in \mathcal{U}$, $t \in \mathcal{T}$. Note that the column $\mathbf{x}_u/\mathbf{s}_u$ of \mathbf{X}/\mathbf{S} , correspond to the training sequence injected by controller u .

B. Steady State Bus Voltages

The steady-state voltages $v_n(t)$ of all buses in slot t are collected in the $T \times N$ steady state bus-voltage matrix \mathbf{V} , defined as $[\mathbf{V}]_{t,n} = v_n(t)$, $n \in \mathcal{N}$, $t \in \mathcal{T}$. To characterize \mathbf{V} in terms of \mathbf{X} , \mathbf{S} and θ , we use Proposition 1 and establish the following result:

Proposition 2. *The steady state of DC MG during the training epoch is characterized by the implicit power balance equation:*

$$\text{vec}(\Omega(\mathbf{V}, \mathbf{X}, \mathbf{S}, \theta)) = \mathbf{0}_{NT}, \quad (16)$$

$$\Omega = \left(\mathbf{S} \mathbf{D}(\mathbf{g}) \mathbf{Q} + \frac{1}{x^2} \mathbf{1}_T (\mathbf{d}^{\text{ca}})^\top \right) \odot \mathbf{V} \odot \mathbf{V} + (\mathbf{V} \mathbf{Y}) \odot \mathbf{V} - \left((\mathbf{S} \odot \mathbf{X}) \mathbf{D}(\mathbf{g}) \mathbf{Q} - \frac{1}{x} \mathbf{1}_T (\mathbf{d}^{\text{cc}})^\top \right) \odot \mathbf{V} + \mathbf{1}_T (\mathbf{d}^{\text{cp}})^\top. \quad (17)$$

$$\Upsilon = \begin{bmatrix} \mathbf{O}_U^\top (\mathbf{Q} \otimes \mathbf{S}^\top) \mathbf{D}^2(\text{vec}(\mathbf{V})) - \mathbf{O}_U^\top (\mathbf{Q} \otimes (\mathbf{S}^\top \odot \mathbf{X}^\top)) \mathbf{D}(\text{vec}(\mathbf{V})) \\ \frac{1}{x^2} (\mathbf{I}_N \otimes \mathbf{1}_T^\top) \mathbf{D}^2(\text{vec}(\mathbf{V}^\top)) \\ \frac{1}{x} (\mathbf{I}_N \otimes \mathbf{1}_T^\top) \mathbf{D}(\text{vec}(\mathbf{V})) \\ \mathbf{I}_N \otimes \mathbf{1}_T^\top \\ \mathbf{O}_{\dim(\psi)}^\top (\mathbf{A}^\top \otimes \mathbf{A}^\top) (\mathbf{I}_N \otimes \mathbf{V}^\top) \mathbf{D}(\text{vec}(\mathbf{V})) \end{bmatrix}^\top. \quad (19)$$

$$\begin{aligned} \Gamma = 2\mathbf{D} \left((\mathbf{Q}^\top \otimes \mathbf{S}) \mathbf{O}_U \mathbf{g} + \frac{1}{x^2} (\mathbf{I}_N \otimes \mathbf{1}_T) \mathbf{d}^{\text{ca}} \right) \mathbf{D}(\text{vec}(\mathbf{V})) - \mathbf{D} \left((\mathbf{Q}^\top \otimes (\mathbf{S} \odot \mathbf{X})) \mathbf{O}_U \mathbf{g} - \frac{1}{x} (\mathbf{I}_N \otimes \mathbf{1}_T) \mathbf{d}^{\text{cc}} \right) \\ + \mathbf{D}((\mathbf{Y} \otimes \mathbf{I}_T) \text{vec}(\mathbf{V})) + \mathbf{D}(\text{vec}(\mathbf{V})) (\mathbf{Y} \otimes \mathbf{I}_T). \end{aligned} \quad (23)$$

where $\Omega : \mathbb{V}^{\dim(\mathbf{V})} \times \mathbb{X}^{\dim(\mathbf{X})} \times \mathbb{S}^{\dim(\mathbf{S})} \times \mathbb{R}^{\dim(\theta)} \mapsto \mathbf{0}_{T \times N}$, $[\Omega]_{t,n} = \omega_n(t)$, $n \in \mathcal{N}$, $t \in \mathcal{T}$ is given in (17).¹⁰

The power balance equation (16) reflects the requirement to keep the system balanced and stable in each slot. We impose $x_u(t) \in \mathbb{X}$, $s_u(t) \in \mathbb{S}$ yielding $v_n(t) \in \mathbb{V}$, for each $u \in \mathcal{U}$, $n \in \mathcal{N}$, $t \in \mathcal{T}$, i.e., we choose the perturbation signals within the respective feasibility sets such that in each slot in the training epoch the MG is in a valid (albeit suboptimal) operating point. Upon closer inspection of Ω as function of θ , we obtain the following result:

Proposition 3. Ω is linear in the parameter vector θ :

$$\text{vec}(\Omega) = \Upsilon \theta, \quad (18)$$

where the $NT \times \dim(\theta)$ matrix Υ is given in (19).

C. Measurement Vectors

Controller $k \in \mathcal{U}_m$, $m \in \mathcal{N}$, measures the m -th column \mathbf{v}_m of \mathbf{V} during the training epoch. We denote the noisy measurement obtained by controller k in slot t with $w_k(t)$, which is the average of $\phi_S(\tau - \tau^*)$ voltage samples collected during the steady state period of slot t :

$$w_k(t) = v_m(t) + z_k(t), \quad (20)$$

where $z_k(t)$ is the additive noise. The measurements are collected in the $T \times U$ bus-voltage measurements matrix \mathbf{W} , $[\mathbf{W}]_{t,u} = w_u(t)$, $u \in \mathcal{U}$, $t \in \mathcal{T}$, satisfying:

$$\mathbf{W} = \mathbf{V} \mathbf{Q}^\top + \mathbf{Z}, \quad (21)$$

where \mathbf{Z} is $T \times U$ matrix containing the noise terms. The k -th column of \mathbf{W} , i.e., \mathbf{w}_k , contains the measurements collected by controller k during the training period. We further assume that $\text{vec}(\mathbf{Z})$ is a zero-mean Gaussian random vector, thus, the probability density function (pdf) of $\text{vec}(\mathbf{W})$ becomes:

$$\rho(\text{vec}(\mathbf{W}); \theta) = \mathbf{N}(\text{vec}(\mathbf{V} \mathbf{Q}^\top), \Sigma). \quad (22)$$

where Σ is the $UT \times UT$ covariance matrix of $\text{vec}(\mathbf{Z})$.

¹⁰We omit denoting explicitly the dependence of Ω on $\mathbf{V}, \mathbf{X}, \mathbf{S}, \theta$.

V. GENERATION, DEMAND AND TOPOLOGY ESTIMATION

This section derives an efficient and unbiased estimator of the unknown parameter vector θ_{-k} , denoted with $\hat{\theta}_{-k}$, for any $k \in \mathcal{U}$. We start by deriving an iterative and efficient MLE algorithm for the benchmark case of *fully known* bus voltages measurement matrix \mathbf{W} and characterize its performance using the CRLB information inequality (Section V-A). The benchmark solution serves as motivation for the developments in Section V-B, where we derive the estimator for the case in which each controller k has access only to its local measurements \mathbf{w}_k in \mathbf{W} .

A. The Case of Fully Known \mathbf{W}

Assume that \mathbf{X} , \mathbf{S} and \mathbf{W} are fully known to controller $k \in \mathcal{U}$. The availability of \mathbf{W} to each controller corresponds to the scenario where an external communication network is available, through which each DER disseminates the local measurements to other DERs.

1) *Sufficient Excitation*: Let $\Upsilon_{-k} = \nabla_{\theta_{-k}} \text{vec}(\Omega)$ denote the $NT \times \dim(\theta_{-k})$ Jacobian of $\text{vec}(\Omega)$ w.r.t. θ_{-k} . Similarly, let $\Gamma = \nabla_{\text{vec}(\mathbf{V})} \text{vec}(\Omega)$ denote the $NT \times NT$ Jacobian of $\text{vec}(\Omega)$ w.r.t. $\text{vec}(\mathbf{V})$, given in (23). When \mathbf{W} is known, the following conditions are sufficient for θ_{-k} to be uniquely identifiable:

$$\text{rank}(\Gamma) = NT, \quad (24)$$

$$\text{rank}(\Upsilon_{-k}) = \dim(\theta_{-k}), \quad (25)$$

for every $k \in \mathcal{U}$. The sufficient excitation conditions provide practical design requirements for the minimal length of the training epoch, i.e., $T \geq N^{-1} \dim(\theta_{-k})$ and the properties of the training matrices, i.e., $\text{rank}(\mathbf{X}) = U$ and $\text{rank}(\mathbf{S}) = U$, which are easily satisfied by making the training sequences \mathbf{x}_u , \mathbf{s}_u , $u \in \mathcal{U}$ orthogonal, i.e., designing them according to the principles of, e.g., binary Walsh-Gold or Hadamard sequences.

2) *Maximum Likelihood Estimator*: Let $\ln \rho(\text{vec}(\mathbf{W}); \theta)$ denote the joint log-likelihood function of $\text{vec}(\mathbf{V})$ and θ_{-k}

$$\mathbf{R}_T^T \boldsymbol{\lambda} = (\boldsymbol{\Gamma}^{(j)} (\mathbf{R}_T^T \boldsymbol{\Sigma}^{-1} \mathbf{R}_T)^{-1} (\boldsymbol{\Gamma}^{(j)})^T)^{-1} (\boldsymbol{\Upsilon}^{(j)} \boldsymbol{\theta} + (\boldsymbol{\Gamma}^{(j)})^T ((\boldsymbol{\Sigma}^{-\frac{1}{2}} \mathbf{R}_T)^\dagger \boldsymbol{\Sigma}^{-\frac{1}{2}} \text{vec}(\mathbf{W}) - \text{vec}(\mathbf{V}^{(j)}))), \quad (36)$$

$$\begin{aligned} \boldsymbol{\theta}_{-k} = & -((\boldsymbol{\Upsilon}_{-k}^{(j)})^T (\boldsymbol{\Gamma}^{(j)} (\mathbf{R}_T^T \boldsymbol{\Sigma}^{-1} \mathbf{R}_T)^{-1} (\boldsymbol{\Gamma}^{(j)})^T)^{-1} \boldsymbol{\Upsilon}_{-k}^{(j)})^{-1} (\boldsymbol{\Upsilon}_{-k}^{(j)})^T (\boldsymbol{\Gamma}^{(j)} (\mathbf{R}_T^T \boldsymbol{\Sigma}^{-1} \mathbf{R}_T)^{-1} (\boldsymbol{\Gamma}^{(j)})^T)^{-1} \\ & \times (\mathbf{v}_k^{(j)} g_k + (\boldsymbol{\Gamma}^{(j)})^T ((\boldsymbol{\Sigma}^{-\frac{1}{2}} \mathbf{R}_T)^\dagger \boldsymbol{\Sigma}^{-\frac{1}{2}} \text{vec}(\mathbf{W}) - \text{vec}(\mathbf{V}^{(j)}))), \end{aligned} \quad (37)$$

$$\begin{aligned} \text{vec}(\mathbf{V}) = & (\boldsymbol{\Sigma}^{-\frac{1}{2}} \mathbf{R}_T)^\dagger \boldsymbol{\Sigma}^{-\frac{1}{2}} \text{vec}(\mathbf{W}) - (\mathbf{R}_T^T \boldsymbol{\Sigma}^{-1} \mathbf{R}_T)^{-1} (\boldsymbol{\Gamma}^{(j)})^T (\boldsymbol{\Gamma}^{(j)} (\mathbf{R}_T^T \boldsymbol{\Sigma}^{-1} \mathbf{R}_T)^{-1} (\boldsymbol{\Gamma}^{(j)})^T)^{-1} \\ & \times (\boldsymbol{\Upsilon}^{(j)} \boldsymbol{\theta} + (\boldsymbol{\Gamma}^{(j)})^T ((\boldsymbol{\Sigma}^{-\frac{1}{2}} \mathbf{R}_T)^\dagger \boldsymbol{\Sigma}^{-\frac{1}{2}} \text{vec}(\mathbf{W}) - \text{vec}(\mathbf{V}^{(j)}))). \end{aligned} \quad (38)$$

for given $\text{vec}(\mathbf{W})$. Then, the MLE of $\boldsymbol{\theta}_{-k}$ is the globally optimal solution to [27], [28]:

$$\begin{aligned} \min_{\text{vec}(\mathbf{V}), \boldsymbol{\theta}_{-k}} \{ & -\ln \rho(\text{vec}(\mathbf{W}); \boldsymbol{\theta}) \}, \quad (26) \\ \text{s.t. } & (\mathbf{Q} \otimes \mathbf{I}_T) \text{vec}(\boldsymbol{\Omega}) = \mathbf{0}_{UT}. \end{aligned}$$

Denote $\mathbf{R}_T = \mathbf{Q} \otimes \mathbf{I}_T$ for notational convenience. Since $\text{vec}(\boldsymbol{\Omega})$ is sufficiently differentiable in $\text{vec}(\mathbf{V})$ and $\boldsymbol{\theta}_{-k}$, the constrained optimization problem in (26) can be restated as an unconstrained one with the same set of stationary points, using the Lagrange method [29]:

$$\min_{\text{vec}(\mathbf{V}), \boldsymbol{\theta}_{-k}, \boldsymbol{\lambda}} \left\{ -\ln \rho(\text{vec}(\mathbf{W}); \boldsymbol{\theta}) + \boldsymbol{\lambda}^T \mathbf{R}_T \text{vec}(\boldsymbol{\Omega}) \right\}, \quad (27)$$

where $\boldsymbol{\lambda}$ is UT vector of multipliers. Under Gaussian noise assumption, see (22), the joint log-likelihood obtains the form:

$$\ln \rho(\text{vec}(\mathbf{W}); \boldsymbol{\theta}) \propto -\frac{1}{2} \|\boldsymbol{\Sigma}^{-\frac{1}{2}} (\text{vec}(\mathbf{W}) - \mathbf{R}_T \text{vec}(\mathbf{V}))\|_2^2. \quad (28)$$

The Karush-Kuhn-Tucker (KKT) conditions [29] are sufficient for existence of stationary point of the objective in (27), yielding the following system of equations:

$$\mathbf{R}_T^T \boldsymbol{\Sigma}^{-1} (\text{vec}(\mathbf{W}) - \mathbf{R}_T \text{vec}(\mathbf{V})) - \boldsymbol{\Gamma}^T \mathbf{R}_T^T \boldsymbol{\lambda} = \mathbf{0}_{NT}, \quad (29)$$

$$\boldsymbol{\Upsilon}_{-k}^T \mathbf{R}_T^T \boldsymbol{\lambda} = \mathbf{0}_{\dim(\boldsymbol{\theta}_{-k})}, \quad (30)$$

$$\text{vec}(\boldsymbol{\Omega}) = \mathbf{0}_{NT}. \quad (31)$$

To find a solution to the above non-linear system, in the following we develop simple and computationally efficient iterative algorithm [28].

3) Iterative Algorithm with Partially Linearized Objective:

Let $\text{vec}(\mathbf{V}^{(j)})$ and $\boldsymbol{\theta}_{-k}^{(j)}$ denote the estimates of $\text{vec}(\mathbf{V})$ and $\boldsymbol{\theta}_{-k}$ obtained in the j -th iteration. We expand $\text{vec}(\boldsymbol{\Omega})$ in Taylor's series and neglect the second order terms:

$$\text{vec}(\boldsymbol{\Omega}) \approx \boldsymbol{\Upsilon}^{(j)} \boldsymbol{\theta} + \boldsymbol{\Gamma}^{(j)} (\text{vec}(\mathbf{V}) - \text{vec}(\mathbf{V}^{(j)})), \quad (32)$$

with $\boldsymbol{\Upsilon}^{(j)}$ and $\boldsymbol{\Gamma}^{(j)}$ evaluated at the current iterates $\text{vec}(\mathbf{V}^{(j)})$ and $\boldsymbol{\theta}_{-k}^{(j)}$. Using the linear approximation (32) in (27), applying the KKT conditions, and solving for $\boldsymbol{\theta}_{-k}$, $\boldsymbol{\lambda}$ and $\text{vec}(\mathbf{V})$, we obtain the following result:

Proposition 4. Consider the following system of equations:

$$\mathbf{R}_T^T \boldsymbol{\Sigma}^{-1} (\text{vec}(\mathbf{W}) - \mathbf{R}_T \text{vec}(\mathbf{V})) - (\boldsymbol{\Gamma}^{(j)})^T \mathbf{R}_T^T \boldsymbol{\lambda} = \mathbf{0}_{NT}, \quad (33)$$

$$(\boldsymbol{\Upsilon}_{-k}^{(j)})^T \mathbf{R}_T^T \boldsymbol{\lambda} = \mathbf{0}_{\dim(\boldsymbol{\theta}_{-k})}, \quad (34)$$

$$\boldsymbol{\Upsilon}^{(j)} \boldsymbol{\theta} + \boldsymbol{\Gamma}^{(j)} (\text{vec}(\mathbf{V}) - \text{vec}(\mathbf{V}^{(j)})) = \mathbf{0}_{NT}. \quad (35)$$

If (24) and (25) are satisfied in $\boldsymbol{\theta}_{-k}^{(j)}$, $\text{vec}(\mathbf{V}^{(j)})$, the unique solution to the system (33)-(35) w.r.t. $\mathbf{R}_T^T \boldsymbol{\lambda}$, $\boldsymbol{\theta}_{-k}$ and $\text{vec}(\mathbf{V})$ is given by (37), (36) and (38), respectively.

We use the result of Proposition 4 to develop an iterative algorithm for finding stationary point of (27):

- 1) set $j = 0$ and initialize $\boldsymbol{\theta}_{-k}$ and $\text{vec}(\mathbf{V})$ with $\boldsymbol{\theta}_{-k}^{(0)}$ and $\text{vec}(\mathbf{V}^{(0)})$, respectively;
- 2) evaluate $\boldsymbol{\Upsilon}^{(j)}$ and $\boldsymbol{\Gamma}^{(j)}$ at $\boldsymbol{\theta}_{-k}^{(j)}$, $\text{vec}(\mathbf{V}^{(j)})$ using (19) and (23), respectively;
- 3) compute $\boldsymbol{\theta}_{-k}^{(j+1)}$ and $\text{vec}(\mathbf{V}^{(j+1)})$ using (37) and (38), respectively;
- 4) evaluate the distances:

$$\begin{aligned} \varepsilon_{\boldsymbol{\theta}}^{(j+1)} &= \|\boldsymbol{\theta}_{-k}^{(j+1)} - \boldsymbol{\theta}_{-k}^{(j)}\|, \\ \varepsilon_{\mathbf{V}}^{(j+1)} &= \|\text{vec}(\mathbf{V}^{(j+1)}) - \text{vec}(\mathbf{V}^{(j)})\|; \end{aligned}$$

- 5) if $\varepsilon_{\boldsymbol{\theta}}^{(j+1)}$ and $\varepsilon_{\mathbf{V}}^{(j+1)}$ meet predefined smallness criteria, stop the algorithm and declare $\boldsymbol{\theta}_{-k}^{(j+1)}$ to be the ML estimate of $\boldsymbol{\theta}_{-k}$;
- 6) otherwise, increase j by 1 and go back to step 2).

To apply the above algorithm, each controller should know the covariance matrix $\boldsymbol{\Sigma}$ up to a scaling factor.

The initialization of the algorithm is the crucial step for finding good estimates of $\boldsymbol{\theta}_{-k}$. Consider the original system of equations (29)-(31); a straightforward solution is:

$$\text{vec}(\mathbf{V}) = (\boldsymbol{\Sigma}^{-\frac{1}{2}} \mathbf{R}_T)^\dagger \boldsymbol{\Sigma}^{-\frac{1}{2}} \text{vec}(\mathbf{W}), \quad (39)$$

$$\mathbf{R}_T^T \boldsymbol{\lambda} = \mathbf{0}_{NT}, \quad (40)$$

$$\boldsymbol{\theta}_{-k} = -\boldsymbol{\Upsilon}_{-k}^\dagger \mathbf{v}_k g_k, \quad (41)$$

where $\boldsymbol{\Upsilon}$ is evaluated in $\text{vec}(\mathbf{V})$ given by (39) and \mathbf{v}_k is the k -th column of $\boldsymbol{\Upsilon}$. (39) and (41) are unbiased but not efficient estimators of $\text{vec}(\mathbf{V})$ and $\boldsymbol{\theta}_{-k}$, respectively, and they can be used to initialize the iterative algorithm. In this regard, the iterations serve to tune and refine the initial estimates (39) and (41), further reducing the estimation error.

4) *Performance:* Relevant performance metric that quantifies the estimation error of $\hat{\boldsymbol{\theta}}_{-k}$ is the $\dim(\boldsymbol{\theta}_{-k}) \times \dim(\boldsymbol{\theta}_{-k})$ Mean Squared Error matrix, defined as:

$$\text{MSE}(\hat{\boldsymbol{\theta}}_{-k}) = \mathbb{E}_{\text{vec}(\mathbf{W})} \left\{ \|\hat{\boldsymbol{\theta}}_{-k} - \boldsymbol{\theta}_{-k}\|_2^2 \right\}. \quad (42)$$

Note that the averaging in (42) is performed w.r.t. the distribution of $\text{vec}(\mathbf{W})$ for fixed $\boldsymbol{\theta}_{-k}$. We bound the MSE matrix of $\hat{\boldsymbol{\theta}}_{-k}$ using the following result:

Proposition 5. The MSE matrix of the ML estimator $\hat{\theta}_{-k}$ is bounded from below through the Cramer-Rao inequality:

$$\text{MSE}(\hat{\theta}_{-k}) \succeq (\Upsilon_{-k}^T (\Gamma^{-1})^T \mathbf{R}_T^T \Sigma^{-1} \mathbf{R}_T \Gamma^{-1} \Upsilon_{-k})^{-1}. \quad (43)$$

The right-hand side in (43) is evaluated at the true values θ and $\text{vec}(\mathbf{V})$. The bound is asymptotically tight [27]; it can be shown that, in high signal-to-noise ratio regimes, the proposed iterative algorithm converges to stationary points with MSE matrix equal to the inverse of the FIM.

B. The Case when the Controllers have Only Local Knowledge

Next, consider the situation when controller $k \in \mathcal{U}_m$ knows only local bus voltage measurements, stored in the k -th column of \mathbf{W} , i.e., $\mathbf{w}_k = \mathbf{V}\mathbf{e}_m + \mathbf{z}_k$ where \mathbf{e}_m is the k -th column of \mathbf{Q}^T , see (6). Evidently, the MLE (26) in this case is not well-conditioned and does not converge to any meaningful solution, since the number of linearly independent equality constraints is at most $T < \dim(\text{vec}(\mathbf{V})) = NT$.¹¹ Thus, in the case when controller k does not have any knowledge of remote buses voltages, the system is *not observable* and θ_{-k} cannot be uniquely identified in classical sense.

Motivated by the framework introduced in Section V-A, we propose sequential-type of solution that organizes the slots into two consecutive *training phases*: (i) phase 0, i.e., *measurement* phase, and (ii) phase 1, also referred to as *communication* phase. The idea is to use the available slots in phase 1 to disseminate the local steady state voltage measurements acquired in phase 0 to remote controllers via amplitude modulation of the perturbation signals. Thus, interpreting the causal relation between the perturbation signals and the induced bus voltage deviations in phase 1 as the input-output equation on an *implicit, all-to-all* communication channel allows us to mimic the case of fully known measurement matrix and use the framework developed in Section V-A.¹² Nevertheless, since each controller relies only on the measurements stored in \mathbf{w}_k to run the computations, the proposed solution can be viewed as a completely decentralized take on (26) when external communication system is not available.

1) *Training Phases*: The temporal organization of the proposed training protocol is depicted in Fig. 5. The time slots in the training epoch are divided into two consecutive groups, i.e., phase 0 and phase 1. Phase 0 comprises T_0 slots, indexed in $\mathcal{T}_0 = \{0, \dots, T_0 - 1\}$, which are further organized into B consecutive *blocks*; the number of slots in each block is $L_0 \geq 0$, such that $BL_0 = T_0$. We write $\mathcal{T}_0 = \cup_{b \in \mathcal{B}} \mathcal{T}_0(b)$ where $\mathcal{B} = \{0, \dots, B - 1\}$ and the disjoint subsets $\mathcal{T}_0(b) = \{bL_0, \dots, (b+1)L_0 - 1\}$, $b \in \mathcal{B}$ are the block-wise index spaces for the slots in phase 0. Phase 1 comprises the remaining $T_1 = T - T_0$ time slots indexed in $\mathcal{T}_1 = \{T_0, \dots, T - 1\}$;

¹¹The only case where \mathbf{w}_k is sufficient to estimate θ_{-k} is $\dim(\text{vec}(\mathbf{V})) = T$, i.e., $N = 1$ corresponding to single bus MG. This case has been considered separately in [20].

¹²The all-to-all nature of the implicit channel allows each controller to listen to *all* other controllers within the MG, i.e., each controller is *connected* to all other controllers; this helps to avoid using distributed Gauss-Newton techniques based on information diffusion and consensus protocols that require iterative exchange of information [30]–[32] to solve the decentralized identification problem.

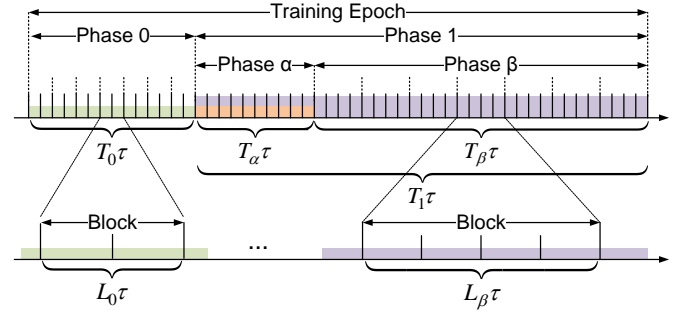


Fig. 5. Proposed training epoch protocol.

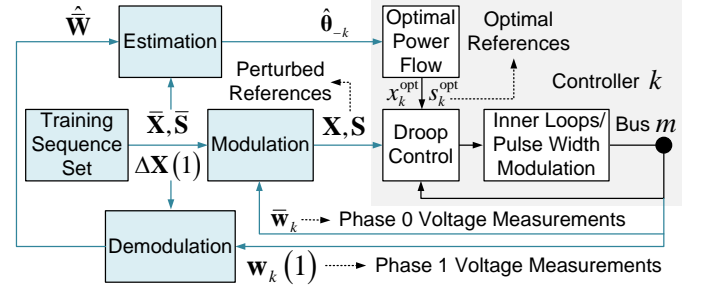


Fig. 6. Architecture of the proposed primary controller in steady state.

it is further split into two separate phases, see Fig. 5. The first T_α slots, indexed with $t \in \mathcal{T}_\alpha = \{T_0, \dots, T_0 + T_\alpha - 1\}$, form phase α , which we refer to as *channel estimation* phase. Finally, the remaining $T_\beta = T - T_0 - T_\alpha$ slots, indexed in $\mathcal{T}_\beta = \{T_0 + T_\alpha, \dots, T - 1\}$ form phase β , i.e., the *modulation* phase where the actual transfer of information takes place. Phase β is further split into B block, each formed by L_β consecutive time slots. Similarly as in phase 0, we have $\mathcal{T}_\beta = \cup_{b \in \mathcal{B}} \mathcal{T}_\beta(b)$ where $\mathcal{B} = \{0, \dots, B - 1\}$ and $\mathcal{T}_\beta(b) = \{T_0 + T_\alpha + bL_\beta, \dots, T_0 + T_\alpha + (b+1)L_\beta - 1\}$, $b \in \mathcal{B}$.

Before proceeding with a detailed description of each of the phases, we introduce notation corresponding to phase-wise and block-wise partition of the matrices \mathbf{X} , \mathbf{S} , \mathbf{V} and \mathbf{W} . For instance, the matrix \mathbf{V} can be partitioned as $\mathbf{V} = [\mathbf{V}^T(0), \mathbf{V}^T(1)]^T$. Similarly $\mathbf{V}(1) = [\mathbf{V}^T(\alpha), \mathbf{V}^T(\beta)]^T$. The $T_0 \times N$ matrix $\mathbf{V}(0)$ is defined as $[\mathbf{V}(0)]_{t,n} = v_n(t)$, $n \in \mathcal{N}$, $t \in \mathcal{T}_0$ and comprises the steady state bus voltages during phase 0; $\mathbf{V}(1)$, $\mathbf{V}(\alpha)$ and $\mathbf{V}(\beta)$ are defined similarly. $\mathbf{V}(0)$ and $\mathbf{V}(\beta)$ can be further partitioned block-wise. For instance $\mathbf{V}(0) = [\mathbf{V}^T(0;0), \dots, \mathbf{V}^T(0;B-1)]^T$ where the $L_\beta \times N$ matrix $\mathbf{V}^T(0;b)$ is defined as $[\mathbf{V}^T(0;b)]_{t,n} = v_n(t)$, $n \in \mathcal{N}$, $t \in \mathcal{T}_\beta(b)$, $b \in \mathcal{B}$; analogous notation applies for $\mathbf{V}(\beta)$. We use $\Sigma = \sigma^2 \mathbf{I}_{UT}$ in the rest of the paper as it simplifies the notation without losing generality.

2) *Primary Control Perturbation Law*: The general architecture of the proposed primary controller is illustrated in Fig. 6. We adopt the following form for the reference voltage perturbation signals:

$$x_u(t) = \tilde{x}_u + \pi_u(t) \Delta x_u(t), \quad (44)$$

for $u \in \mathcal{U}$, $t \in \mathcal{T}$, where $\Delta x_u(t)$ is the reference voltage perturbation, satisfying $|\Delta x_u(t)| = 1$ and $\pi_u(t)$ is the positive amplitude. \tilde{x}_u together with \tilde{s}_u , $u \in \mathcal{U}$ define the nominal

operating point with steady state voltage response denoted by \tilde{v}_n , $n \in \mathcal{N}$. In practice, the nominal operating point usually corresponds to the optimal values x_u^{opt} , s_u^{opt} from the previous OPF epoch, or, it may be a predefined combination, determined a priori; in any case, \tilde{x}_u and \tilde{s}_u (and hence \tilde{v}_n) are fixed and controller u knows \tilde{v}_n via noisy version \tilde{w}_u , obtained before the beginning of the training epoch. The training matrix \mathbf{X} can be written as follows:

$$\mathbf{X} = \mathbf{1}_T \tilde{\mathbf{x}}^\top + \mathbf{\Pi} \odot \Delta \mathbf{X}, \quad (45)$$

where $\tilde{\mathbf{x}} = [\tilde{x}_1, \dots, \tilde{x}_U]^\top$, $[\mathbf{\Pi}]_{t,u} = \pi_u(t)$, $[\Delta \mathbf{X}]_{t,u} = \Delta x_u(t)$, $u \in \mathcal{U}$, $t \in \mathcal{T}$. The reference voltage perturbation matrix $\Delta \mathbf{X}$ is known to each controller.

3) *Phase 0 (collecting the measurements)*: The perturbation signals in phase 0 follow block-wise excitation law, i.e., in each block $b \in \mathcal{B}$, the controllers move the system to a predefined operating point, defined by the pairs $\bar{x}_u(b)$, $\bar{s}_u(b)$, $u \in \mathcal{U}$ with steady state voltage response $\bar{v}_n(b)$, $n \in \mathcal{N}$; the system stays there for L_0 consecutive slots. Thus, the perturbation signals are:

$$x_u(t) = \bar{x}_u(b), \quad (46)$$

$$s_u(t) = \bar{s}_u(b), \quad (47)$$

for $u \in \mathcal{U}$, $t \in \mathcal{T}_0(b)$, $b \in \mathcal{B}$. The $T_0 \times U$ training matrices $\mathbf{X}(0)$, $\mathbf{S}(0)$ can be written as follows:

$$\mathbf{X}(0) = (\mathbf{I}_B \otimes \mathbf{1}_{L_0}) \bar{\mathbf{X}}, \quad (48)$$

$$\mathbf{S}(0) = (\mathbf{I}_B \otimes \mathbf{1}_{L_0}) \bar{\mathbf{S}}, \quad (49)$$

where $[\bar{\mathbf{X}}]_{b,u} = \bar{x}_u(b)$ and $[\bar{\mathbf{S}}]_{b,u} = \bar{s}_u(b)$, $u \in \mathcal{U}$, $b \in \mathcal{B}$. The $U \times B$ matrices $\bar{\mathbf{X}}$, $\bar{\mathbf{S}}$ are assumed to be a priori known to all controllers.

The $T_0 \times N$ bus voltages matrix $\mathbf{V}(0)$ obtains the form:

$$\mathbf{V}(0) = (\mathbf{I}_B \otimes \mathbf{1}_{L_0}) \bar{\mathbf{V}}, \quad (50)$$

where $[\bar{\mathbf{V}}]_{b,n} = \bar{v}_n(b)$, $n \in \mathcal{N}$, $b \in \mathcal{B}$. During block b , controller $u \in \mathcal{U}_n$ measures the steady-state bus voltage $v_n(t) = \bar{v}_n(b)$, $t \in \mathcal{T}_0(b)$ and computes the average:

$$\bar{w}_u(b) = \bar{v}_n(b) + \frac{1}{L_0} \sum_{t \in \mathcal{T}_0(b)} z_u(t). \quad (51)$$

or, compactly:

$$\bar{\mathbf{W}} = (\mathbf{I}_B \otimes \mathbf{1}_{L_0})^\dagger \mathbf{W}(0), \quad (52)$$

where $\bar{\mathbf{W}} = [\bar{w}_u(b)]_{b,u}$, $u \in \mathcal{U}$, $b \in \mathcal{B}$; the pdf of $\text{vec}(\bar{\mathbf{W}})$ is:

$$\mathcal{N}\left(\text{vec}(\bar{\mathbf{V}}\mathbf{Q}^\top), \frac{\sigma^2}{L_0} \mathbf{I}_{UB}\right). \quad (53)$$

In phase 0, controller k learns the k -th column of $\bar{\mathbf{W}}$, i.e., $\bar{\mathbf{w}}_k$. We introduce phase 1, where controller k disseminates $\bar{\mathbf{w}}_k$ to remote controllers via modulation of the amplitudes $\pi_u(t)$, $t \in \mathcal{T}_1$ and, in the same time, learns the remaining columns $\bar{\mathbf{w}}_u$, $u \neq k$, obtaining full knowledge of the block-wise measurement matrix $\bar{\mathbf{W}}$, as described next.

4) *Phase 1 (communication)*: We assume that the reference voltage deviation amplitudes are relatively small w.r.t. the nominal reference voltage:

$$\frac{\pi_u(t)}{\tilde{x}_u} \ll 1, \quad (54)$$

for $u \in \mathcal{U}$ and $t \in \mathcal{T}_1$. We obtain the following linear approximation:

$$\mathbf{V}(1) \approx \mathbf{1}_{T_1} \tilde{\mathbf{v}}^\top + (\mathbf{\Pi}(1) \odot \Delta \mathbf{X}(1)) \mathbf{H}, \quad (55)$$

where $\tilde{\mathbf{v}} = [\tilde{v}_1, \dots, \tilde{v}_N]^\top$ and $\mathbf{H} = -\nabla_{\mathbf{x}}^\top \omega(\nabla_{\mathbf{v}}^{-1} \omega)^\top$, evaluated in the nominal operating point, is the $U \times N$ real *channel matrix*. The model (55) defines the input-output relation of a real, linear, synchronous, full-duplex, decentralized, multiple-input multiple-output communication system, with channel matrix \mathbf{H} that remains fixed in phase 1 since it does not depend on $\Delta \mathbf{X}(1)$. We use this model to design sequential-type of transceiver. Specifically, we split phase 1 into two separate phases: phase α and phase β . In phase α , the controllers estimates the corresponding row of the channel matrix. Afterward, in phase β the controllers modulate the information acquired in phase 0 into the reference voltage perturbation amplitudes.

To obtain compact and insightful expressions, without losing generality, we restrict the columns of $\Delta \mathbf{X}(\alpha)$ and $\Delta \mathbf{X}(\beta; b)$, $b \in \mathcal{B}$ to be orthogonal and zero mean:

$$\Delta \mathbf{X}^\top(\alpha) \mathbf{1}_{T_\alpha} = \mathbf{0}_U, \quad \Delta \mathbf{X}^\top(\alpha) \Delta \mathbf{X}(\alpha) = \delta_\alpha^2 \mathbf{I}_U, \quad (56)$$

$$\Delta \mathbf{X}^\top(\beta; b) \mathbf{1}_{L_\beta} = \mathbf{0}_U, \quad \Delta \mathbf{X}^\top(\beta; b) \Delta \mathbf{X}(\beta; b) = \delta_\beta^2 \mathbf{I}_U, \quad (57)$$

where $\delta_\alpha^2 = \|\Delta \mathbf{x}_u(\alpha)\|_2^2 \leq T_\alpha$, $\delta_\beta^2 = \|\Delta \mathbf{x}_u(\beta; b)\|_2^2 \leq L_\beta$, $u \in \mathcal{U}$, $b \in \mathcal{B}$.

Phase α (channel estimation): In this phase, the perturbation amplitudes are given by:

$$\pi_u(t) = \pi_\alpha, \quad (58)$$

for $u \in \mathcal{U}_n$, $n \in \mathcal{N}$, $t \in \mathcal{T}_\alpha$. $\pi_\alpha > 0$ is *known* constant. Replacing the above in (55), the m -th column of the matrix $\mathbf{V}(\alpha)$, observed by controller k in phase α can be approximated as:

$$\mathbf{v}_m(\alpha) \approx \tilde{v}_m \mathbf{1}_{T_\alpha} + \pi_\alpha \Delta \mathbf{X}(\alpha) \mathbf{h}_k, \quad (59)$$

where \mathbf{h}_k is the k -th column of the matrix $\mathbf{H}\mathbf{Q}^\top$. Replacing $\mathbf{v}_m(\alpha)$ and \tilde{v}_m with $\mathbf{w}_k(\alpha)$ and \tilde{w}_k , respectively, the estimator $\hat{\mathbf{h}}_k$ is the solution to the following linear least squares (LLSE) problem:

$$\min_{\mathbf{h}_k} \left\| \pi_\alpha \Delta \mathbf{X}(\alpha) \mathbf{h}_k - \mathbf{w}_k(\alpha) + \tilde{w}_k \mathbf{1}_{T_\alpha} \right\|_2^2. \quad (60)$$

which, under assumptions (56) and (57) gives:

$$\hat{\mathbf{h}}_k = \frac{1}{\pi_\alpha \delta_\alpha^2} \Delta \mathbf{X}^\top(\alpha) \mathbf{w}_k(\alpha) \sim \mathcal{N}\left(\mathbf{h}_k, \frac{\sigma^2}{\pi_\alpha^2 \delta_\alpha^2} \mathbf{I}_U\right). \quad (61)$$

Phase β (modulation and demodulation): In this phase, the reference voltage deviations have the following amplitudes:

$$\pi_u(t) = \pi_\beta(\bar{w}_u(b) + \varphi_u), \quad (62)$$

for $u \in \mathcal{U}$, $b \in \mathcal{B}$, $t \in \mathcal{T}_\beta(b)$; $\pi_\beta \geq 0$ and $\varphi_u \geq 0$ are *known* constants. Replacing (62) in (55), the m -th column of

$$\Delta \bar{\Sigma}_k = \frac{\sigma^2}{\pi_\alpha^2 \delta_\alpha^2} \mathbf{D}^{-1}((\mathbf{I}_U \otimes \mathbf{1}_B) \mathbf{h}_k) \mathbf{D} \left(\sum_{b \in \mathcal{B}} (\mathbf{I}_U \otimes \mathbf{e}_b) \mathbf{Q} \bar{\mathbf{v}}(b) \right) (\mathbf{I}_U \otimes \mathbf{1}_B \mathbf{1}_B^T) \left(\sum_{b \in \mathcal{B}} (\mathbf{I}_U \otimes \mathbf{e}_b) \mathbf{Q} \bar{\mathbf{v}}(b) \right) \mathbf{D}^{-1}((\mathbf{I}_U \otimes \mathbf{1}_B) \mathbf{h}_k). \quad (71)$$

the matrix $\mathbf{V}(\beta; b)$, observed by controller k in block b of phase β , can be approximated as:

$$\mathbf{v}_m(\beta; b) \approx \tilde{v}_m \mathbf{1}_{L_\beta} + \pi_\beta \Delta \mathbf{X}(\beta; b) \mathbf{D}(\mathbf{h}_k) (\bar{\mathbf{w}}(b) + \boldsymbol{\varphi}), \quad (63)$$

for $b \in \mathcal{B}$, where $\boldsymbol{\varphi} = [\varphi_1, \dots, \varphi_U]^T$. Note that $\bar{\mathbf{w}}^T(b)$ is the b -th row of $\bar{\mathbf{W}}$ that contains the bus voltages measured by the controllers during block b in phase 0. Replacing $\mathbf{v}_m(\beta; b)$, \tilde{v}_m and \mathbf{h}_k with $\mathbf{w}_k(\beta; b)$, \tilde{w}_k and $\hat{\mathbf{h}}_k$, respectively, the estimate of $\bar{\mathbf{w}}(b)$ is the solution to the LSE problem:

$$\min_{\bar{\mathbf{w}}(b)} \left\| \pi_\beta \Delta \mathbf{X}(\beta; b) \mathbf{D}(\hat{\mathbf{h}}_k) (\bar{\mathbf{w}}(b) + \boldsymbol{\varphi}) - \mathbf{w}_k(\beta; b) + \tilde{w}_k \mathbf{1}_{L_\beta} \right\|_2^2, \quad (64)$$

for $b \in \mathcal{B}$. At the end of phase β , the local estimate $\hat{\bar{\mathbf{W}}}_k$, under assumptions (56) and (57), can be written as:

$$\hat{\bar{\mathbf{W}}}_k = \frac{1}{\pi_\beta \delta_\beta^2} \left(\sum_{b \in \mathcal{B}} \mathbf{e}_b \mathbf{w}_k^T(\beta; b) \Delta \mathbf{X}(\beta; b) \right) \odot (\mathbf{1}_B \hat{\mathbf{h}}_k^T) - \mathbf{1}_B \boldsymbol{\varphi}^T. \quad (65)$$

The controllers will be able to uniquely resolve all transmissions in phases α and β if $\text{rank}(\Delta \mathbf{X}(\alpha; b)) = U$ and $\text{rank}(\Delta \mathbf{X}(\beta; b)) = U$, i.e., $T_\alpha \geq U$, $L_\beta \geq U$.

5) *MLE and CRLB*: Let $\bar{\boldsymbol{\Omega}} = (\mathbf{I}_B \otimes \mathbf{1}_{L_0})^\dagger \boldsymbol{\Omega}(0)$ denote the $B \times U$ power balance matrix, corresponding to phase 0. Similarly, let $\bar{\boldsymbol{\Upsilon}}$ and $\bar{\boldsymbol{\Gamma}}$ denote the Jacobians of $\bar{\boldsymbol{\Omega}}$ w.r.t., $\boldsymbol{\theta}$ and $\text{vec}(\bar{\mathbf{V}})$, respectively.¹³ The local estimate $\hat{\bar{\mathbf{W}}}_k$ is sufficient to uniquely identify $\boldsymbol{\theta}_{-k}$ using the MLE developed in Section V-A when the following sufficient excitation conditions are satisfied:

$$\text{rank}(\bar{\boldsymbol{\Gamma}}) = NB, \quad (66)$$

$$\text{rank}(\bar{\boldsymbol{\Upsilon}}_{-k}) = \dim(\boldsymbol{\theta}_{-k}). \quad (67)$$

The sequential estimator (65) treats the estimated channel gain $\hat{\mathbf{h}}_k$ as perfectly known; hence, we use the conditional pdf of $\text{vec}(\hat{\bar{\mathbf{W}}}_k)$ to run the MLE algorithm:

$$\mathcal{N} \left(\text{vec}(\bar{\mathbf{V}} \mathbf{Q}^T), \frac{\sigma^2}{L_0} \mathbf{I}_{UB} + \frac{\sigma^2}{\pi_\beta^2 \delta_\beta^2} \mathbf{D}^{-2}((\mathbf{I}_U \otimes \mathbf{1}_B) \hat{\mathbf{h}}_k) \right). \quad (68)$$

The performance of the MLE is characterized with the following proposition:

Proposition 6. *The MSE matrix of the ML estimator $\hat{\boldsymbol{\theta}}_{-k}$ obtained by processing $\hat{\bar{\mathbf{W}}}_k$ is bounded from below through the Cramer-Rao inequality:*

$$\text{MSE}(\hat{\boldsymbol{\theta}}_{-k}) \succeq (\bar{\boldsymbol{\Upsilon}}_{-k}^T (\bar{\boldsymbol{\Gamma}}^{-1})^T \mathbf{R}_B^T \bar{\Sigma}_k^{-1} \mathbf{R}_B \bar{\boldsymbol{\Gamma}}^{-1} \bar{\boldsymbol{\Upsilon}}_{-k})^{-1}. \quad (69)$$

$\bar{\Sigma}_k$ is the covariance matrix of $\text{vec}(\hat{\bar{\mathbf{W}}}_k)$ and is given by the approximation:

$$\bar{\Sigma}_k \approx \frac{\sigma^2}{L_0} \mathbf{I}_{UB} + \frac{\sigma^2}{\pi_\beta^2 \delta_\beta^2} \mathbf{D}^{-2}((\mathbf{I}_U \otimes \mathbf{1}_B) \mathbf{h}_k) + \Delta \bar{\Sigma}_k, \quad (70)$$

¹³ $\bar{\boldsymbol{\Omega}}$, $\bar{\boldsymbol{\Upsilon}}$ and $\bar{\boldsymbol{\Gamma}}$ are given by (17), (19) and (23), respectively, after replacing \mathbf{X} , \mathbf{S} , \mathbf{V} and T with $\bar{\mathbf{X}}$, $\bar{\mathbf{S}}$, $\bar{\mathbf{V}}$ and B .

where $\Delta \bar{\Sigma}_k$ is given in (71).

The above result captures the effect of phase 1 upon $\hat{\boldsymbol{\theta}}_{-k}$. Specifically, the initial uncertainty in $\bar{\mathbf{W}}$, represented with the first term in (70) (see also (53)), is increased due to measurement noise in phase β and channel uncertainty induced in phase α , captured with the last two terms in (70). We further see that the uncertainty increase depends inversely on $\pi_\alpha^2 \delta_\alpha^2$ and $\pi_\beta^2 \delta_\beta^2$, (i.e., the total energy “injected” by each controller in phases α and β), and can be reduced by increasing either the duration of phase 1 or increasing the dynamic range of the reference voltage amplitudes.

We conclude this section by deriving simple upper bound on the number of DERs U that can be simultaneously supported by the proposed solution, subject to constraint on the duration of the training epoch:

$$T = B(L_0 + L_\beta) + T_\alpha \geq \frac{U+1}{N} \dim(\boldsymbol{\theta}_{-k}) + U, \quad (72)$$

where we used $L_0 \geq 1$, $T_\alpha \geq U$, $L_\beta \geq U$ and the sufficient excitation condition (67). The right-hand side in (72) is maximized for $U = N$, i.e., the special case when each DER is modeled as separate bus; hence, we obtain the following lower bound:

$$T \geq \frac{1}{2} U^2 + 5U + \frac{5}{2} - \frac{1}{U}. \quad (73)$$

For instance, if the total duration of the training phase is required to be no longer than 1 minute, then, for slot durations of 50 milliseconds (including the transient time), the maximum number of DERs (buses) that can be supported by the proposed solution is $U = 45$, requiring at least 1200 time slots.

VI. NUMERICAL EVALUATION

A. Simulation Description

MG parameters: The rated voltage of the system and the lower threshold are $x = 400$ V and $v_{\min} = 390$ V, respectively. We fix $U = N$ and $\mathbf{Q} = \mathbf{I}_N$. The generation capacities, load demands (in watts) and the line admittances (in siemens) are: $\mathbf{g} = g \mathbf{1}_U^T$, $g = 5$, $\mathbf{d}^{\text{ca}} = d^{\text{ca}} \mathbf{1}_N$, $d^{\text{ca}} = 1.5$, $\mathbf{d}^{\text{cc}} = d^{\text{cc}} \mathbf{1}_N$, $d^{\text{cc}} = 1$, $\mathbf{d}^{\text{cp}} = d^{\text{cp}} \mathbf{1}_N$, $d^{\text{cp}} = 0$ and $y_{n,m} \equiv y$, $y = 1$, $n, m \in \mathcal{N}$. The nominal operating point is $\tilde{x}_u = x$, $\tilde{s}_u = (v_{\min}(x - v_{\min}))^{-1}$, $u \in \mathcal{U}$. The sampling frequency and standard deviation of the sampling noise of PECs' ADCs are $\phi_S = 50$ kHz and $\sigma_S = 0.1$ V/sample. We consider two distribution network topologies, see Fig. 7: 1)

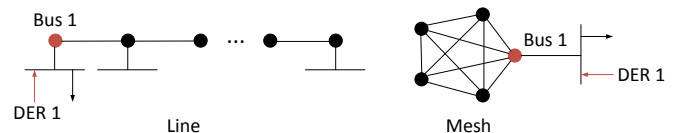


Fig. 7. Simulated DC MG distribution topologies.

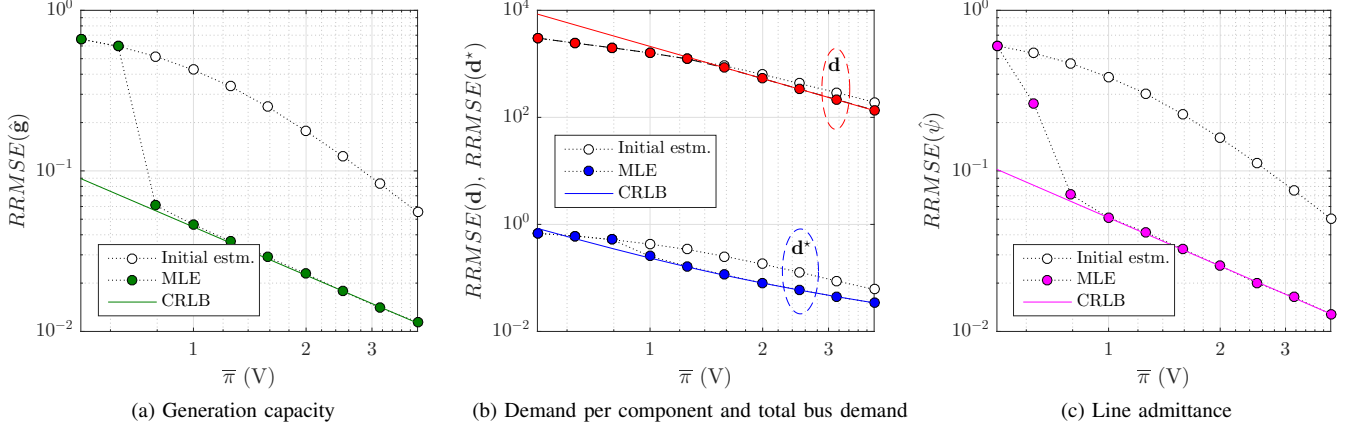


Fig. 8. Standard deviation of the estimation error per component of the vectors \mathbf{g} , \mathbf{d} , \mathbf{d}^* and ψ : the number of DERs is $U = 5$ and they are connected in line, see Fig. 7, the reference voltage deviation amplitudes in phase 0 and phase 1 are equal, i.e., $\pi = \bar{\pi}$.

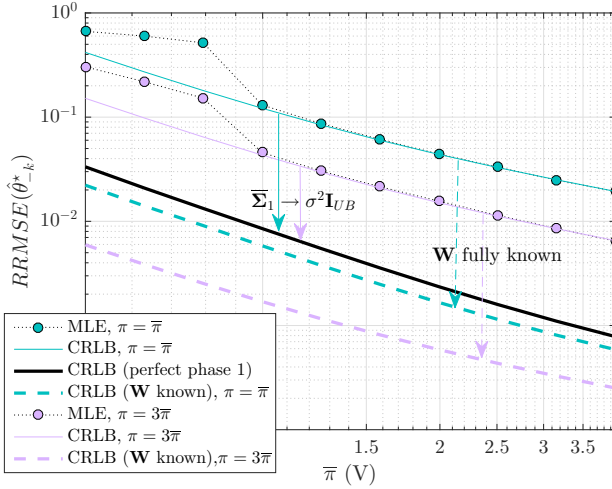


Fig. 9. Attainable and non-attainable performance bounds per component of the parameter vector $\theta_{-k}^* = [\mathbf{g}^T, (\mathbf{d}^*)^T, \psi^T]^T$: the number of DERs is $U = 5$ and they are connected in line, see Fig. 7.

line (i.e., cut ring), where all buses are connected to two other buses except for buses $n = 1$ and $n = U$ that are connected to a single bus each, and 2) mesh (i.e., all-to-all), where each bus is connected to all other buses.¹⁴

Training epoch parameters: The number of slots and the steady state duration of a slot are fixed to $T = 600$ and $\tau = 50$ milliseconds, respectively. The noise is white Gaussian with standard deviation $\sigma_S(\sqrt{\phi_{ST}})^{-1}$. In phases α and β we use:

$$\pi_\alpha = \pi, \pi_\beta = \pi 0.25(x - v_{\min}), \varphi_u = \tilde{w}_u, \quad (74)$$

$$\Delta \mathbf{x}_u(\alpha) = \Delta \mathbf{x}_u(\beta; b) = \mathbf{e}_u \otimes [1, -1]^T, \quad (75)$$

$$T_\alpha = 2U, L_\beta = 2U, \delta_\alpha = \delta_\beta = \sqrt{2}, \quad (76)$$

¹⁴The line topology represents an isolated feeder from the distribution grid or a typical uninterrupted power supply system in parallel configuration [2], [3]. The mesh topology on the other hand corresponds to a Kron-reduced version of an equivalent sparse system with many load buses; in this case, Kron reduction is applied to isolate the DER buses which results in a system of reduced order with full admittance matrix [33].

for $u \in \mathcal{U}$; the durations of phase α and β are kept fixed and π is used to control the amplitude of the reference voltage perturbations. In phase 0, we fix $L_0 = 1$ and the reference voltage perturbation sequence $\Delta \mathbf{x}_u(0)$ comprises the first B elements of the column at position $2^{u-1} + 1$ in the binary Walsh matrix; the duration B and the perturbation amplitudes $\pi_u(t)$ in phase 0 are set as:

$$B = \left\lfloor \frac{T - 2U}{1 + 2U} \right\rfloor, \pi_u(t) = \bar{\pi}, \quad (77)$$

for $u \in \mathcal{U}$, $t \in \mathcal{T}_0$. The droop slope is kept equal to the nominal value $s_u(t) = \bar{s}$.

Performance metric: We use a Relative Root MSE (RRMSE) metric, defined as:

$$\text{RRMSE}(\cdot) = \|\cdot\|_2^{-1} \sqrt{\text{trace}(\text{MSE}(\cdot))}, \quad (78)$$

where “ \cdot ” stands for either scalar or vector. When applied to a scalar, i.e., individual components of the parameter vector, RRMSE quantifies the standard deviation of the estimates around the true values of that particular component, whereas, if applied to a vector, the RRMSE is interpreted as the standard deviation of the estimation error per component of the vector (e.g., $\text{RRMSE}(\hat{\mathbf{g}})$ and $\text{RRMSE}(\hat{\mathbf{d}})$ quantify the average estimation error per generation capacity and load demand component, respectively).

B. Results

We evaluate the performance of the proposed solution in terms of RRMSE for different components in the parameter vector and for varying number of DERs, from the perspective of controller 1 connected to bus 1. Empty markers correspond to the initial estimate that initializes the MLE, obtained via (41), while filled markers correspond to the MLE $\hat{\theta}_{-k}$ after the algorithm converges and attains the CRLB as expected [27]. It can be observed that the generation capacities, Fig. 8(a), and the line admittances, Fig. 8(c), can be identified with high precision. In contrast, the RRMSE of the load demands of individual components, Fig. 8(b), is several orders of magnitude higher and might prove to be unsatisfactory. However, in

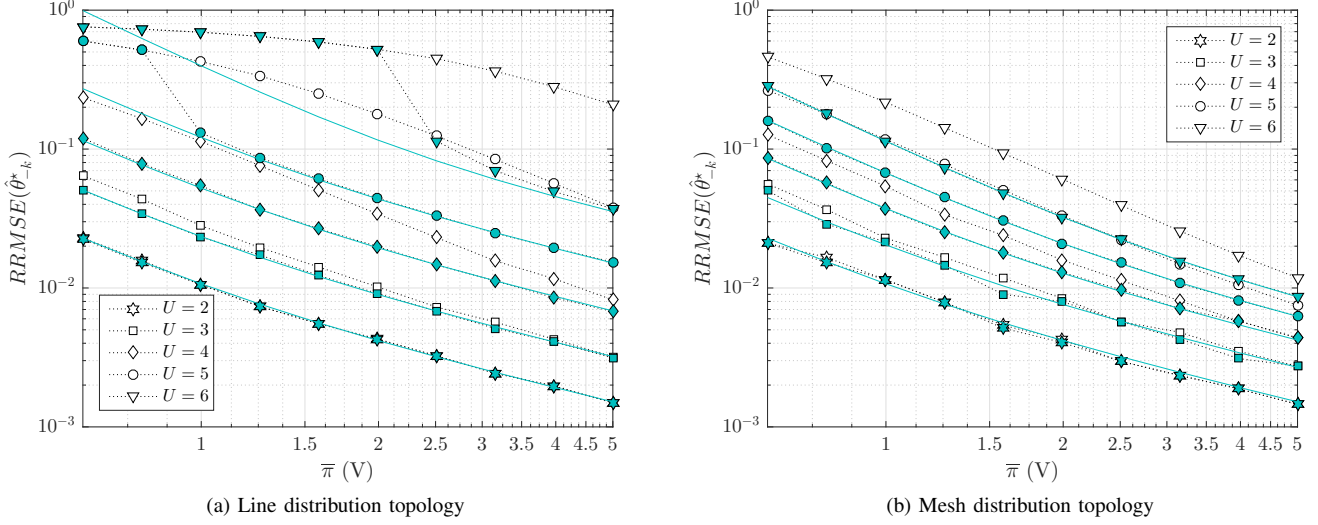


Fig. 10. Scalability evaluation per component of the parameter vector $\theta_{-k}^* = [\mathbf{g}^T, (\mathbf{d}^*)^T, \psi^T]$: the number of DERs U is variable, the reference voltage deviation amplitudes in phase 0 and phase 1 are equal, i.e., $\pi = \bar{\pi}$.

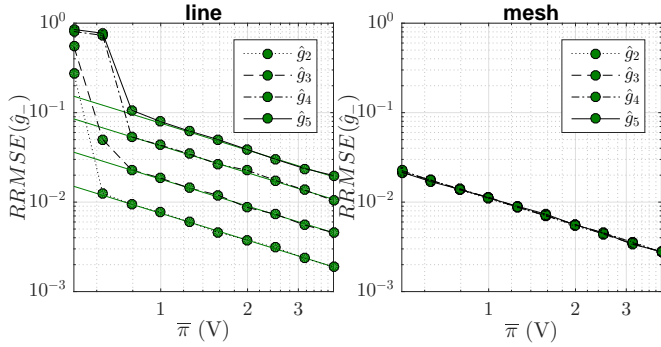


Fig. 11. Scalability evaluation for individual components in \mathbf{g} : the number of DERs is $U = 5$, the reference voltage deviation amplitudes in phase 0 and phase 1 are equal, i.e., $\pi = \bar{\pi}$.

many upper control layer applications, detailed knowledge on the load component demands is not necessary and knowing only the total bus load demand $d_n^* = d_n^{ca} + d_n^{cc} + d_n^{cp}$ is sufficient [5]–[8]; in such case, an estimate of the total load demand vector $\mathbf{d}^* = [d_1^*, \dots, d_N^*]^T$ can be obtained from $\hat{\mathbf{d}}$ via $\hat{\mathbf{d}}^* = [\mathbf{I}_N, \mathbf{I}_N, \mathbf{I}_N]\hat{\mathbf{d}}$. Fig. 8(b) shows that $\hat{\mathbf{d}}^*$ can be identified with a precision comparable to the one achieved for the generation capacities and line admittances.

Next, we observe that the performance of the MLE can be always bounded from above via the performance of the initial estimate, which is unbiased but suboptimal, see Fig. 8 and Fig. 10. This insight becomes practically viable when $N \rightarrow 1$, as evident in Fig. 10, i.e., when the performance of the initial estimate approaches the CRLB; in such case, there is no performance gain from applying the iterative MLE.¹⁵ Fig. 9 depicts the CRLB corresponding to the case when the second and third term in (70) are 0, referred to as “perfect

phase 1” CRLB; it represents the best performance the MLE can achieve in absence of external communication enabler, for given phase 0 (i.e., for given duration B and deviation amplitude $\bar{\pi}$) in the limit when the total energy “injected” by each controller in phase 1, is infinite i.e., (i) the durations satisfy $T_\alpha \rightarrow \infty$ and $L_\beta \rightarrow \infty$, or (ii) the deviation amplitude satisfies $\pi \rightarrow \infty$. Hence, the “perfect phase 1” CRLB is asymptotically achievable. As a comparison, Fig. 9 also shows the CRLB for the benchmark case. This bound can be attained only when controller 1 knows all columns of \mathbf{W} (i.e., an external communication network is available). It is interesting to note that, as the total amount of energy “injected” in phase 1 increases, by increasing π from $\bar{\pi}$ to $3\bar{\pi}$, the performance of the MLE approaches the “perfect phase 1” CRLB, but the gap to the benchmark case remains (approximately) fixed.

Fig. 10 investigates the performance of the framework for increasing number of DERs. In general, the performance tends to deteriorate as U increases, which is expected. Also, the MLE performs better for mesh topologies compared to the ring-like configurations. This observation is valid in general: namely, the MLE achieves lower estimation errors in DC MGs with distribution systems that are more strongly connected. The above conclusion is a direct corollary of the following general observation: the estimation accuracy is higher for DERs, loads and lines that are connected to controller 1 via higher equivalent admittance. The effect can be seen in Fig. 11, where we see that when the DERs follow line topology, the RRMSE of individual capacity estimates deteriorates for the DERs which are not directly connected to bus 1. This further motivates development of distributed upper control layer applications, where each controller requires only knowledge of the DERs and loads that are within its closest neighborhood, as these can be learned with the highest precision.

In summary, the numerical investigations, presented in Figs. 8, 9 and 10 show that in typical LVDC MG settings, the relative estimation error is below 1%, for reference voltage

¹⁵The only case when the initial estimate attains the CRLB corresponds to $N = 1$, i.e., the single bus case. In [20] we show that the solution (41) is the global minimizer of the negative log-likelihood function of θ_{-k} .

deviation amplitudes that are lower than 1% of the rated voltage x of the MG. This confirms the practical applicability of the proposed solution for upper control layer applications.

VII. CONCLUDING REMARKS

We introduced autonomous system identification framework, based on temporary primary control perturbations and iterative MLE estimation for DC MGs without access to an external communication system. The framework is implemented in a decentralized manner within the primary droop controllers of the PECs and enables the controllers to learn i) the generation capacities of power sources, ii) the load demands, and iii) distribution network topology; these parameters determine the steady state bus voltages through a non-linear, implicit model that can be identified. The proposed solution utilizes decentralized training architecture where the primary controllers inject small, amplitude-modulated training sequences that complete the rank of the estimation problem and help regain full system observability. The numerical evaluations verify the analysis and show that the in typical LVDC MG settings, the relative estimation error can as low as 1% with voltage deviation amplitudes smaller than 1% of the rated MG value.

Our on-going investigations focus on (i) modeling θ as stochastic dynamic process and applying Bayesian filtering/prediction techniques to learn/predict its current/future values, (ii) extension to AC and hybrid AC/DC MG systems, (iii) joint co-design of the OPF and training epochs.

REFERENCES

- [1] R. H. Lasseter and P. Paigi, "Microgrid: a conceptual solution," in *2004 IEEE 35th Annual Power Electronics Specialists Conference (IEEE Cat. No. 04CH37551)*, vol. 6, June 2004, pp. 4285–4290 Vol.6.
- [2] L. E. Zubieta, "Are microgrids the future of energy?: Dc microgrids from concept to demonstration to deployment," *IEEE Electrification Magazine*, vol. 4, no. 2, pp. 37–44, June 2016.
- [3] T. Dragicevic, X. Lu, J. C. Vasquez, and J. M. Guerrero, "Dc microgrids; part i: A review of control strategies and stabilization techniques," *IEEE Transactions on Power Electronics*, vol. 31, no. 7, pp. 4876–4891, July 2016.
- [4] C. Jin, P. Wang, J. Xiao, Y. Tang, and F. H. Choo, "Implementation of hierarchical control in dc microgrids," *IEEE Transactions on Industrial Electronics*, vol. 61, no. 8, pp. 4032–4042, Aug 2014.
- [5] S. Moayed and A. Davoudi, "Unifying distributed dynamic optimization and control of islanded dc microgrids," *IEEE Transactions on Power Electronics*, vol. 32, no. 3, pp. 2329–2346, March 2017.
- [6] H. Liang, B. J. Choi, A. Abdrabou, W. Zhuang, and X. S. Shen, "Decentralized economic dispatch in microgrids via heterogeneous wireless networks," *IEEE Journal on Selected Areas in Communications*, vol. 30, no. 6, pp. 1061–1074, July 2012.
- [7] L. Gan and S. H. Low, "Optimal power flow in direct current networks," *IEEE Transactions on Power Systems*, vol. 29, no. 6, pp. 2892–2904, Nov 2014.
- [8] G. B. Giannakis, V. Kekatos, N. Gatsis, S. J. Kim, H. Zhu, and B. F. Wollenberg, "Monitoring and optimization for power grids: A signal processing perspective," *IEEE Signal Processing Magazine*, vol. 30, no. 5, pp. 107–128, Sept 2013.
- [9] P. Chavali and A. Nehorai, "Distributed power system state estimation using factor graphs," *IEEE Transactions on Signal Processing*, vol. 63, no. 11, pp. 2864–2876, June 2015.
- [10] T. Erseghe, S. Tomasin, and A. Vigato, "Topology estimation for smart micro grids via powerline communications," *IEEE Transactions on Signal Processing*, vol. 61, no. 13, pp. 3368–3377, July 2013.
- [11] X. Zhong, L. Yu, R. Brooks, and G. K. Venayagamoorthy, "Cyber security in smart dc microgrid operations," in *2015 IEEE First International Conference on DC Microgrids (ICDCM)*, June 2015, pp. 86–91.
- [12] O. Beg, T. Johnson, and A. Davoudi, "Detection of false-data injection attacks in cyber-physical dc microgrids," *IEEE Transactions on Industrial Informatics*, vol. PP, no. 99, pp. 1–1, 2017.
- [13] S. Galli, A. Scaglione, and Z. Wang, "For the grid and through the grid: The role of power line communications in the smart grid," *Proceedings of the IEEE*, vol. 99, no. 6, pp. 998–1027, June 2011.
- [14] J. Schonberger, R. Duke, and S. D. Round, "Dc-bus signaling: A distributed control strategy for a hybrid renewable nanogrid," *IEEE Transactions on Industrial Electronics*, vol. 53, no. 5, pp. 1453–1460, Oct 2006.
- [15] D. Chen, L. Xu, and L. Yao, "Dc voltage variation based autonomous control of dc microgrids," *IEEE Transactions on Power Delivery*, vol. 28, no. 2, pp. 637–648, April 2013.
- [16] T. L. Vandoorn, B. Renders, L. Degroote, B. Meersman, and L. Van-develde, "Active load control in islanded microgrids based on the grid voltage," *IEEE Transactions on Smart Grid*, vol. 2, no. 1, pp. 139–151, March 2011.
- [17] M. Angelichinoski, C. Stefanovic, P. Popovski, H. Liu, P. C. Loh, and F. Blaabjerg, "Power talk: How to modulate data over a dc micro grid bus using power electronics," in *2015 IEEE Global Communications Conference (GLOBECOM)*, Dec 2015, pp. 1–7.
- [18] M. Angelichinoski, C. Stefanovic, P. Popovski, H. Liu, P. C. Loh, and F. Blaabjerg, "Multiuser communication through power talk in dc microgrids," *IEEE Journal on Selected Areas in Communications*, vol. PP, no. 99, pp. 1–1, 2016.
- [19] M. Angelichinoski, C. Stefanovic, and P. Popovski, "Power talk for multibus dc microgrids: Creating and optimizing communication channels," in *2016 IEEE Global Communications Conference (GLOBECOM)*, Dec 2016, pp. 1–7.
- [20] M. Angelichinoski, A. Scaglione, P. Popovski, and C. Stefanovic, "Distributed estimation of the operating state of a single-bus dc microgrid without an external communication interface," in *2016 IEEE Global Signal and Information Processing Conference (GlobalSIP)*, Dec 2016, pp. 1–4.
- [21] M. Angelichinoski, Č. Stefanović, and P. Popovski, *Modemless Multiple Access Communications Over Powerlines for DC Microgrid Control*. Springer International Publishing, 2016, pp. 30–44.
- [22] A. Vosoughi and A. Scaglione, "Everything you always wanted to know about training: guidelines derived using the affine precoding framework and the crb," *IEEE Transactions on Signal Processing*, vol. 54, no. 3, pp. 940–954, March 2006.
- [23] M. Ciobotaru, R. Teodorescu, P. Rodriguez, A. Timbus, and F. Blaabjerg, "Online grid impedance estimation for single-phase grid-connected systems using pq variations," in *2007 IEEE Power Electronics Specialists Conference*, June 2007, pp. 2306–2312.
- [24] S. Cobres, E. J. Bueno, D. Pizarro, F. J. Rodriguez, and F. Huerta, "Grid impedance monitoring system for distributed power generation electronic interfaces," *IEEE Transactions on Instrumentation and Measurement*, vol. 58, no. 9, pp. 3112–3121, Sept 2009.
- [25] A. B. et al, "Experimental determination of the zip coefficients for modern residential, commercial, and industrial loads," *IEEE Transactions on Power Delivery*, vol. 29, no. 3, pp. 1372–1381, June 2014.
- [26] J. W. Simpson-Porco, F. Drfler, and F. Bullo, "On resistive networks of constant-power devices," *IEEE Transactions on Circuits and Systems II: Express Briefs*, vol. 62, no. 8, pp. 811–815, Aug 2015.
- [27] H. L. V. Trees, *Detection, Estimation, and Modulation Theory: Radar-Sonar Signal Processing and Gaussian Signals in Noise*. Melbourne, FL, USA: Krieger Publishing Co., Inc., 1992.
- [28] H. I. Britt and R. H. Luecke, "The estimation of parameters in nonlinear, implicit models," *Technometrics*, vol. 15, no. 2, pp. 233–247, 1973. [Online]. Available: <http://www.jstor.org/stable/1266984>
- [29] S. Boyd and L. Vandenberghe, *Convex Optimization*. New York, NY, USA: Cambridge University Press, 2004.
- [30] M. Eisen, A. Mokhtari, and A. Ribeiro, "Decentralized quasi-newton methods," *IEEE Transactions on Signal Processing*, vol. 65, no. 10, pp. 2613–2628, May 2017.
- [31] T. H. Chang, M. Hong, and X. Wang, "Multi-agent distributed optimization via inexact consensus admm," *IEEE Transactions on Signal Processing*, vol. 63, no. 2, pp. 482–497, Jan 2015.
- [32] J. Chen and A. H. Sayed, "Diffusion adaptation strategies for distributed optimization and learning over networks," *IEEE Transactions on Signal Processing*, vol. 60, no. 8, pp. 4289–4305, Aug 2012.
- [33] F. Dorfler and F. Bullo, "Kron reduction of graphs with applications to electrical networks," *IEEE Transactions on Circuits and Systems I: Regular Papers*, vol. 60, no. 1, pp. 150–163, Jan 2013.